university of groningen

faculty of science and engineering

Low Surface Brightness Galaxies in the Fornax-Eridanus Supercluster

Pavani Ravichandran

university of groningen / faculty of science and engineering

University of Groningen

Low Surface Brightness Galaxies in the Fornax-Eridanus Supercluster

Master's Thesis

To fulfill the requirements for the degree of
Master of Science in Astronomy
at University of Groningen under the supervision of
Prof. dr. R.F. Peletier (Astronomy, University of Groningen)
and
dr. M.A. Raj (Astronomy, University of Groningen)

Pavani Ravichandran (s5084903)

August 22, 2024

Contents

Abstract

Low surface brightness dwarf galaxies (LSBs) are galaxies with effective surface brightness $\bar{\mu}_{e,g} > 24.2$ mag arcsec^{-2} and are the most abundant galaxies in our Universe. Their diffuse nature makes them susceptible to interactions with nearby galaxies and environment which can affect their morphology and structure. Recent developments in deep, wide-field observations have made it possible to probe LSBs on a large scale. For example, Tanoglidis et al. 2021 performed g, r, i band photometry of LSBs in the Dark Energy Survey (DES) and found that red LSBs tend to cluster in regions that mostly coincide with known galaxy clusters, while blue LSBs dominate the areas outside these groups.

Galaxies in our Universe form a web-like structure called the Cosmic Web, where dense clusters and groups are connected by intermediate-density filaments and walls, separated by very low-density voids. The Fornax-Eridanus supercluster is embedded in the Fornax Wall, connecting the Fornax cluster, Eridanus Supergroup, and the Dorado group. These systems are in the process of merging with nearby groups, providing an opportunity to study the effects of the large-scale environment on galaxies. Recently, Raj et al. 2024 detected the spine (or central axis) of the Fornax Wall and studied the morphology of massive galaxies relative to the spine. They found a morphological segregation, where early-type galaxies highly populated regions close to the spine.

Our objective is to explore the effect of the large-scale environment on LSBs in the Fornax-Eridanus Supercluster. Specifically, we investigate whether LSBs trace the Fornax Wall spine, like massive galaxies do (Raj et al. 2024). We first identify members of the Fornax Wall from the photometric LSB catalog by Tanoglidis et al. 2021 and we divide the population into two groups: i) those within one virial radius of galaxy groups and ii) those outside this radius (pristine galaxies). We then study their distribution within the supercluster. We probe the morphology-density relation and examine galaxy properties such as effective radius, surface brightness, Sérsic index, and stellar mass with respect to their distance from the spine of the Fornax Wall.

Our findings show that red LSBs are located in and near groups close to the Fornax Wall, where they dominate the population, while blue LSBs dominate in the pristine environment. We also find that groups host a population of red LSBs with large effective radius, a characteristic not found in regions far from groups. This indicates that the environment plays a significant role in the formation of large-sized LSBs. This work lays the foundation for future studies that explore in detail the importance of local and large-scale environments in the formation and evolution of LSBs.

1 Introduction

1.1 The Cosmic Web and superclusters

Redshift surveys (e.g., Huchra et al. 1983) and N-body simulations (e.g., Springel et al. 2005b, Vogelsberger et al. 2014) have shown that baryonic and dark matter form large-scale structures (de Lapparent et al. 1986) on scales of Mpc called the Cosmic Web (Bond et al. 1996. The Cosmic Web (see Figure 1) consists of filaments and walls, connecting high-density nodes comprised of clusters and groups of galaxies. These may be separated by extremely low density regions, known as voids.

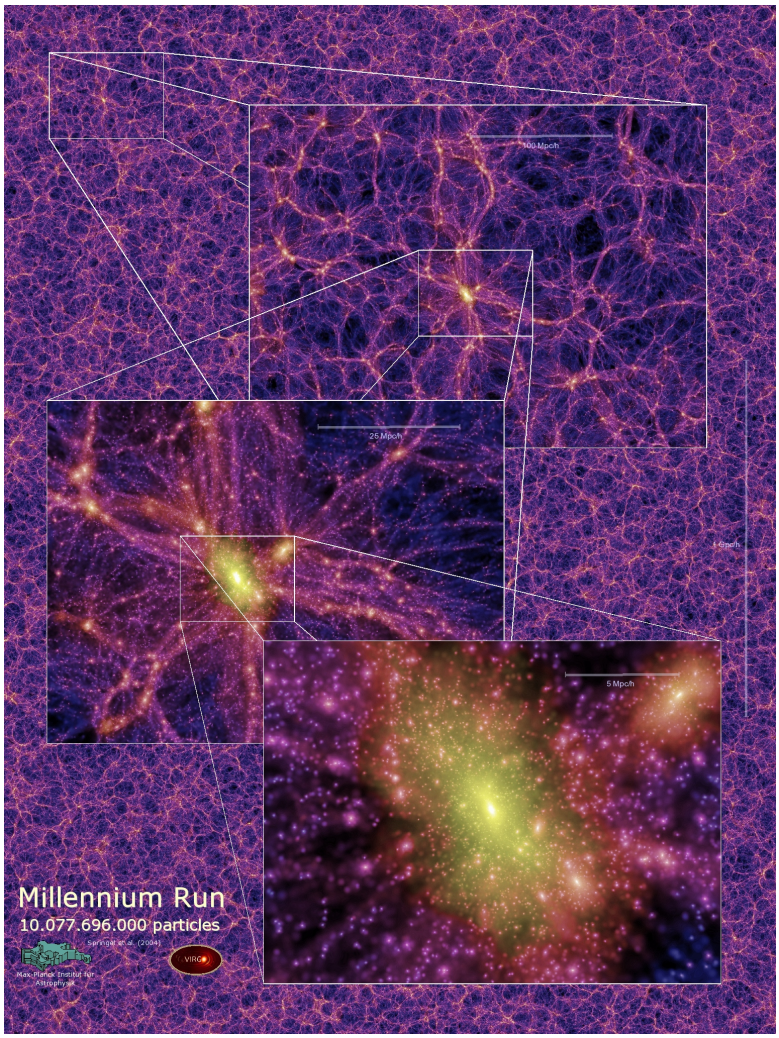

Figure 1: Structures in the Cosmic Web: Poster from the Millennium Simulation Project (Springel et al. 2005a) of the projected dark matter density field for a 15 Mpc/h thick slice of redshift z = 0. The bottom-most tile highlights a node, the middle tile displays filamentary structures around the node, and the top-most tile provides a broad view of the Cosmic Web.

Galaxy evolution is known to depend on the local matter density. In dense regions, galaxies can interact with the local environment and evolve differently compared to those in low density regions. Apart from this, the large-scale environment in which these regions lie also affects the galaxy evolutionary pathways. According to the ΛCDM model (White and Rees 1978), the dark matter halos in

which galaxies reside, merge hierarchically through gravitational interactions. Galaxies and matter flow from low density regions to high density regions. Clusters and groups grow by accreting individual, pairs or entire groups of galaxies. This evolution has been found to depend on their large-scale environment (e.g., Einasto et al. 2012a, Tempel et al. 2009).

Groups, clusters and filaments can be embedded in larger systems called superclusters (de Vaucouleurs 1958) and these superclusters may be situated in walls (Einasto et al. 2010, Einasto et al. 2017). Various studies (e.g., Araya-Melo et al. 2009, Tully et al. 2014, Haines et al. 2018, Einasto et al. 2021) have demonstrated that these massive structures vary significantly in their dynamical states, galaxy compositions, and sizes. The high density cores of superclusters host rich clusters that accrete nearby galaxies while small, poor groups tend to populate other regions (Einasto et al. 2012b). As they are dynamically evolving, studying the impact of dense supercluster regions on galaxies is crucial to understand galaxy formation and evolution, and thus, large-scale structures.

1.2 Formation and evolution of dwarf galaxies

Dwarf galaxies constitute a majority of the galaxy population in the Universe and their low mass and surface brightness makes them highly susceptible to interactions with their surrounding environment. Therefore, they are ideal objects to study the effects of the large-scale environment. In this section, we describe dwarf galaxies and their formation and evolution within environments such as clusters, groups and filaments of a supercluster.

1.2.1 Dwarf galaxies and their classification

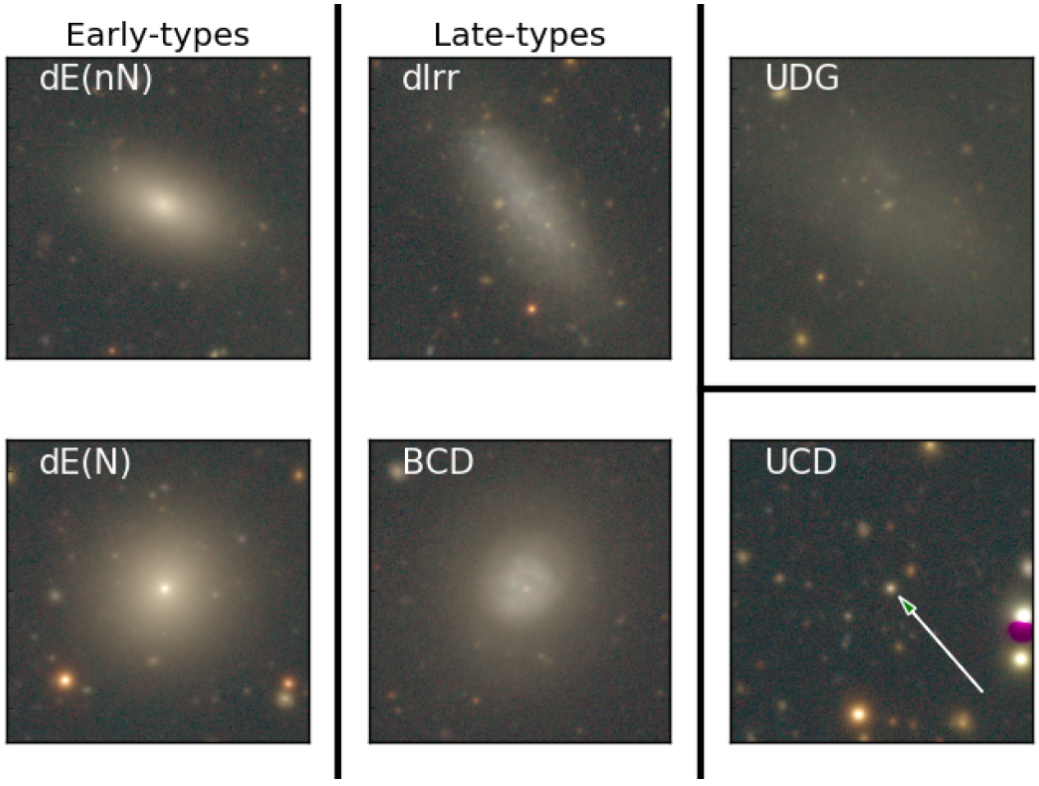

Figure 2: Prototype of dwarf galaxies with different morphology types in the Fornax cluster. Figure adapted from Venhola 2019.

Dwarf galaxies are defined as galaxies with absolute magnitude $M_B > -18$ mag (e.g., Boselli et al. 2008). They exhibit a variety of shapes and internal structures. Like giant galaxies, dwarfs can be classified based on their star formation activity into quiescent early-type dwarfs or gas-rich, star forming late-type dwarfs. Due to the difficulties in observing gas in these faint galaxies, their morphology is usually determined based on optical color, with early-type galaxies appearing red and late-type galaxies appearing blue.

As in Figure 2, dwarf galaxies can be further classified based on their luminosity and appearance (e.g., Sandage and Binggeli 1984, Kormendy and Bender 2012). Early-type galaxies with a smooth spherical appearance are classified as dwarf ellipticals (dEs), while those that also have a disk component are dwarf lenticulars (dS0s). Late-type galaxies are typically dwarf irregulars (dIrrs) and have a clumpy irregular appearance. Further divisions can be based on structural parameters like surface brightness (e.g., UDGs or ultra-diffuse galaxies), nucleation (e.g., dE(N) or nucleated dwarf ellipticals) or their compactness (e.g., BCD or blue compact dwarfs, UCD or ultra-compact dwarfs).

These classifications often reflect different formation or evolutionary mechanisms, some of which are discussed briefly in the following sections.

1.2.2 Cluster environment

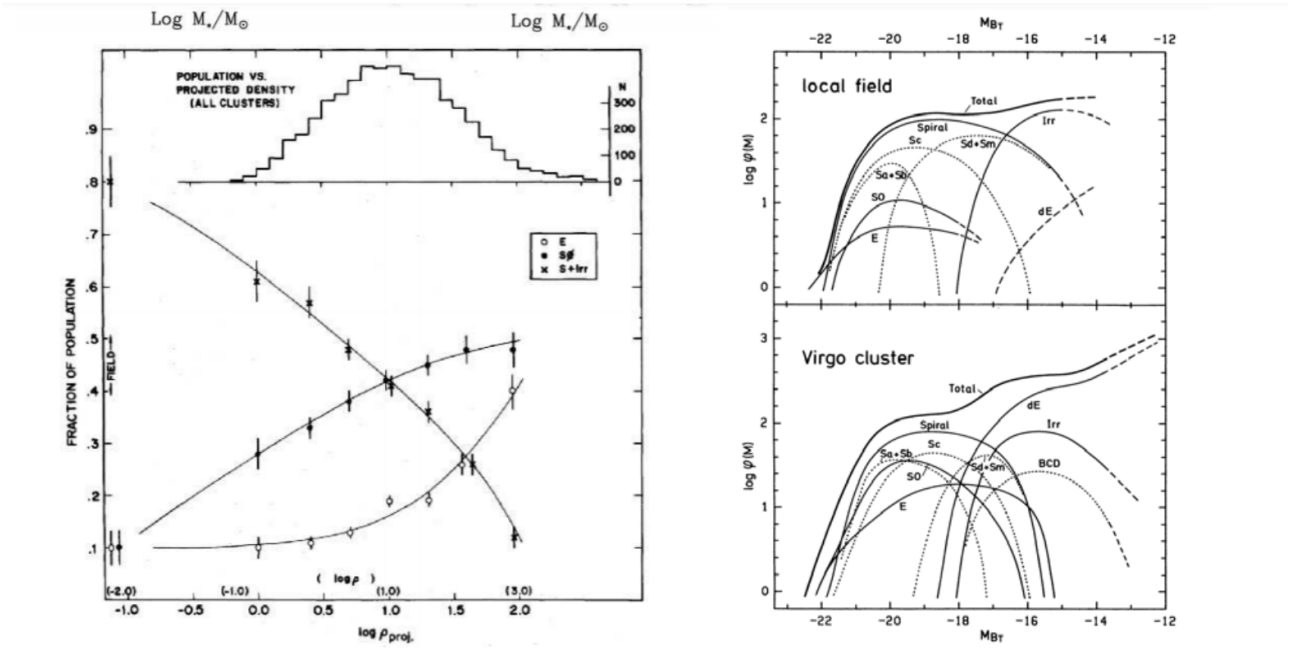

Figure 3: Morphology-density relation observed in galaxy clusters (left); Figure adapted from Dressler 1980. Luminosity function of galaxies with different morphology in low-density fields (top-right) and the Virgo cluster (bottom-right); Figure adapted from Binggeli et al. 1988.

On observing massive galaxies, Dressler 1980 (Figure 3) found that early-type ellipticals and lenticulars are more abundant in clusters than late-type spirals and irregulars. Similarly, in the case of dwarf galaxies, it has been established that dEs are observed much more in high density environments than in the field (Su et al. 2022, Venhola et al. 2022, Geha et al. 2012,Binggeli et al. 1987). Figure 3 shows the luminosity function of various types of galaxies in the field and the cluster environment.

The Virgo cluster is dominated by dEs, while the field is dominated by dIrrs (or Irr in the figure). The morphology-density relation is more pronounced for dwarfs than for massive galaxies due to their shallow potential wells. For instance, no late-type dwarfs were found in the central region of the Virgo cluster (Binggeli et al. 1987) while blue dwarfs almost exclusively populate isolated environments (Leisman et al. 2017, Geha et al. 2012,Román and Trujillo 2017).

The early-type dwarfs in clusters may have been formed through passive evolution of primordial galaxies (e.g., Wheeler et al. 2017) before being accreted onto the cluster. However, the diversity in structures found in cluster dEs suggests that they have multiple formation channels (e.g., formation of nucleus as discussed by Su et al. 2022). These galaxies often possess gas tails, discs (Lisker et al. 2006) and have prolonged star formation histories (Koleva et al. 2011) similar to late-type dwarfs. These features and the observed morphology-density relation within clusters suggests that they likely form either through mergers (de Rijcke et al. 2005) or through environmental effects on star-forming late-type dwarfs (Kormendy 1985).

When star-forming progenitors from nearby groups and filaments enter the cluster, they can interact with the hot intracluster medium and cluster galaxies. Ram-pressure stripping can remove gas and suppress star formation (Boselli et al. 2008). In some cases, imperfect ram-pressure stripping can move gas to the inner parts, allowing star formation to continue in the center while the outer parts become redder as the stellar population ages (e.g., Mun et al. 2021). Infalling dwarfs can also gravitationally interact with their hosts (e.g., galaxy strangulation; Garling et al. 2020) or other massive galaxies in the cluster (e.g., harrassment; Smith et al. 2015). Tidal interactions can induce morphological changes (like gas tails), strip the stars and gas in dwarfs, effectively quenching their star formation. Interactions with nearby massive galaxies can also expand dwarf galaxies, creating low surface brightness, "puffed up" UDGs (Tremmel et al. 2020).

Although the environmental processes that transform late-type galaxies are most common in clusters, there has been evidence of cluster members that were pre-processed outside. Lisker et al. 2018 observed a group of dEs that were recently accreted by the Virgo cluster. Three dEs in this group showed no signs of recent star formation, suggesting that their star formation was quenched before their accretion into the Virgo cluster (Bidaran et al. 2020). Before their infall, pre-processed galaxies may have belonged to groups or may have entered the clusters from nearby filaments (e.g., Lee et al. 2021) where they may have interacted with the environment. They may also enter from nearby low-density areas such as voids or filament outskirts, retaining some of their original properties (Lee et al. 2021). Several observations support the significant impact of pre-processing such as the presence of quenched galaxies beyond one virial radius of clusters (e.g., Donnari et al. 2021) and diminished star formation activity in late-type galaxies located between one and three virial radius (Haines et al. 2015).

1.2.3 Group and filament environments

Groups are generally considered to be less virialized compared to clusters (Paul et al. 2017), although the distinction between the two is not sharp. In groups, quenching of infalling galaxies by ram-pressure stripping and harrassment are less effective due to the smaller relative velocities and lower densities. As a result, dwarf galaxies in groups can have bluer colors on average compared to cluster galaxies (Venhola et al. 2017). Interactions with the host galaxy and internal processes like feedback might dominate and the galaxies might be more similar to isolated dwarfs than cluster galaxies.

Most of the dwarf galaxies in the filament environment and outside groups are blue, late-type star-

forming dwarfs (e.g., Chung et al. 2021). Although filaments have relatively lower densities, signs of environmental impact on dwarfs have been found. For example, Chung et al. 2021 showed that star-forming dwarfs in some Virgo filaments had enhanced metallicities and suppressed star formation comparable to those in the cluster. Transitional dwarfs (blue-cored dEs) were found in their filament population, and are thought to be formed due to ram-pressure stripping or harrassment (Lisker et al. 2006). These galaxies fit the pre-processing scenario defined previously. However, whether the galaxies in filaments are influenced by the large-scale environment, or just by the local environment and their proximity to massive host galaxies is still unclear.

1.3 Previous studies on the Supercluster-scale

The properties of massive galaxies have been shown to depend on the large-scale environment. Red luminous ellipticals tend to have stronger clustering than blue, faint spirals suggesting a large-scale morphology-density relation (e.g., Skibba et al. 2009, Einasto and Einasto 1987). Groups in the outskirts of supercluster cores were shown to have more late-type galaxies (Einasto et al. 2008). More early-type galaxies were found in dense supercluster cores both in groups and outside groups as compared to other regions (Einasto et al. 2007).

To determine whether these observations are indeed due to large-scale environmental processes and not the local environment or internal mechanisms, a more precise definition of filaments that connect the different groups and clusters is required. Recently, Raj et al. 2024 determined the filamentary structures around the Fornax-Eridanus supercluster and was able to study the position of massive galaxies with respect to the structures. The fraction of early-type and late-type galaxies in groups were found to depend on the distance from the filament spine (central axis), while there were no gradients for both early-type and late-type galaxies outside groups. This suggests that the morphology of massive galaxies in groups depends on the proximity to filaments within the supercluster.

Since dwarf galaxies are more susceptible to their environment than massive galaxies, it can be expected that they show a stronger dependance on large-scale environment. Only a handful of studies exist for dwarf galaxies in a supercluster (e.g., Mahajan et al. 2010, Mahajan et al. 2011, Zanatta et al. 2024) and they have observed a dependance of their morphology on the local environment within a supercluster. This thesis complements the research by Raj et al. 2024 (hereafter, R24) and will be the first of its kind to explore the distribution and morphology of (low surface-brightness) dwarf galaxies in a supercluster using the spine of the wall that the supercluster is embedded in.

1.4 The Fornax-Eridanus supercluster

The closest large-scale structure to the Local Supercluster is the Southern Supercluster (Mitra 1989). It is a long strand of galaxies connecting Cetus, Fornax, Eridanus, Horologium and the Dorado group (de Vaucouleurs 1953, de Vaucouleurs 1956). The Fornax-Eridanus supercluster consists of the Fornax cluster (NGC1399), its infalling group (NGC1316), the Eridanus Supergroup (NGC1407, NGC1302, NGC1332, NGC1395, NGC1398; Brough et al. 2006) and the Dorado Group (NGC1533, NGC1672). The groups in the Fornax and Eridanus regions are found to be merging (Nasonova et al. 2011, Makarov and Karachentsev 2011). Along with NGC1316, smaller pairs and triplets are found to be merging with the Fornax cluster. The groups in the Eridanus region are also predicted to eventually merge with each other (Brough et al. 2006) to form a cluster. Although the Supergroup is still merging, the galaxies in each (sub)group are at different stages of evolution. For example, NGC1407 is considered to be a fossil group because the galaxies within it are mostly early-type (Trentham et al.

2006) while NGC1332 is known to have more star-forming late-type massive galaxies (R24). The Dorado group is in its early evolutionary stage.

The Fornax-Eridanus supercluster is embedded within the Fornax Wall (Fairall et al. 1994). The central axis or the spine of the Fornax Wall is made of four filaments that connects the major groups in the region (see Figure 4). It spans a length of 31 Mpc/h ranging from the distance of 15 Mpc/h to 30 Mpc/h and is the most populated large-scale structure in the surrounding region. It contains $\sim$ 50% of the massive galaxies ($K_s < 12.5$ mag) in the large-scale structures defined by R24 within its neighbourhood radius 3 Mpc h^{-1}.

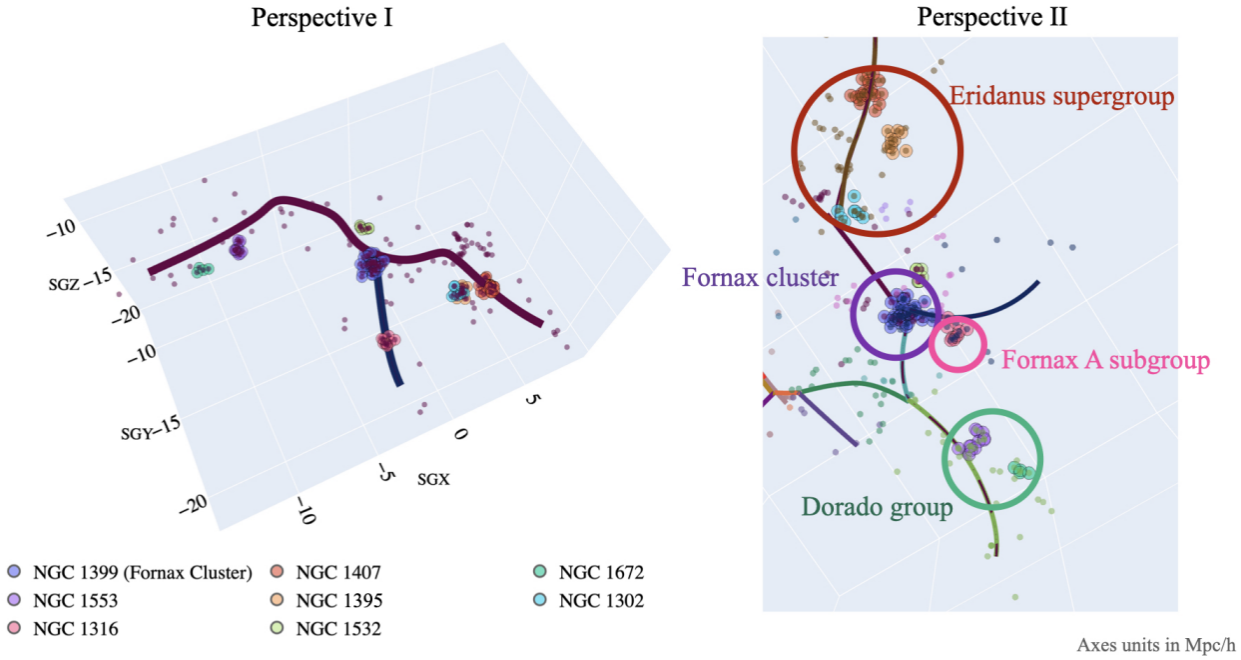

Figure 4: The Fornax Wall in two different perspectives of its 3D location. The spine of the Fornax Wall along with the spine of the filament connecting Fornax A group with the Fornax cluster (left). The major groups and clusters within the Fornax Wall (right). Figure adapted from R24.

Aside from the Fornax Wall, there are other filaments in this region described by R24. A filament connects the Fornax A group with the Fornax cluster (Figure 4). Other filaments connect to the Fornax Wall at the Eridanus Supergroup and close to the Dorado group. The focus of this work will be on the galaxies and groups that belong to the Fornax Wall, with the adjacent structures left for future studies.

1.5 Research Goals

A majority of dwarf galaxies also have low surface brightness ($\bar{\mu}_{e,g} > 24.2$ mag arcsec^{-2}). Recently, a photometric catalog of low-surface brightness galaxies (LSBs) was made and analysed by Tanoglidis et al. 2021 (hereafter, T21) as a part of the Dark Energy Survey (DES) Collaboration. They studied the two-point correlation function (Peebles 1980) which can estimate the clustering in a sample of galaxies. They found that red LSBs have a higher correlation amplitude (more clustering) than their blue counterparts. The difference in clustering between red and blue LSBs was not due to a difference in stellar mass as the correlation function was not dependant on the magnitude of the galaxies. This suggests that environmental effects are responsible for the clustering.

As mentioned in Section 1.3, R24 found that the morphology of massive galaxies was dependant on the distance to the spine of filaments. The groups along a filament had more early-type massive galaxies than the regions outside groups. Different filaments also had differing fractions of early-type massive galaxies. The large-scale processes that cause the morphological segregation in massive galaxies may also be the cause of the clustering of red LSBs observed by T21. Meanwhile, some theoretical studies have shown that the strong clustering of faint red galaxies may be because they are predominantly satellites of massive hosts (Berlind et al. 2005, Wang et al. 2009, Zehavi et al. 2011). The processes that cause this clustering are yet to be determined and, whether the local or the large-scale environment matters is an open question.

The primary goal of this thesis is to identify signs of large-scale environmental effects on LSBs in the Fornax-Eridanus supercluster using the spine of the Fornax Wall determined with massive galaxies by R24. The research aims to establish a foundation for future studies on faint galaxy evolution in superclusters. Specifically, we focus on addressing the following:

a. How are LSBs distributed in the Fornax-Eridanus Supercluster?

b. Do LSBs follow the morphology-density relation on a large-scale, as a function of distance from the Fornax Wall?

c. How are their structural properties affected?

d. Does their evolution depend on their immediate environment or do they depend on the large-scale structure?

2 Data

In order to perform a statistical study on the LSBs of the Fornax Wall, a large, homogeneous and highly complete sample is required. Given the very low surface-brightness, very few LSBs can be found in the wide-field (e.g., Geller et al. 2012, Blanton et al. 2005), therefore a deeper survey is needed. Dark Energy Survey (DES) uses the ground-based Dark Energy Camera (DECam; Flaugher et al. 2015) to obtain deep imaging in the optical SDSS g, r, i, z bands in the Southern Hemisphere. The survey footprint shown in Figure 5, mostly encloses the $\sim$ 1750 sq. deg region (red patch in the figure) used in this thesis, fully including all the Fornax Wall groups. T21 provides a LSB catalog based on DES. We match their catalog with the Fornax Deep Survey dwarf catalog (FDSDC) by Venhola et al. 2018, which has a completeness of $\geq$ 50%. The T21 catalog has nearly $\sim$ 45% of the FDSDC dwarf galaxies.

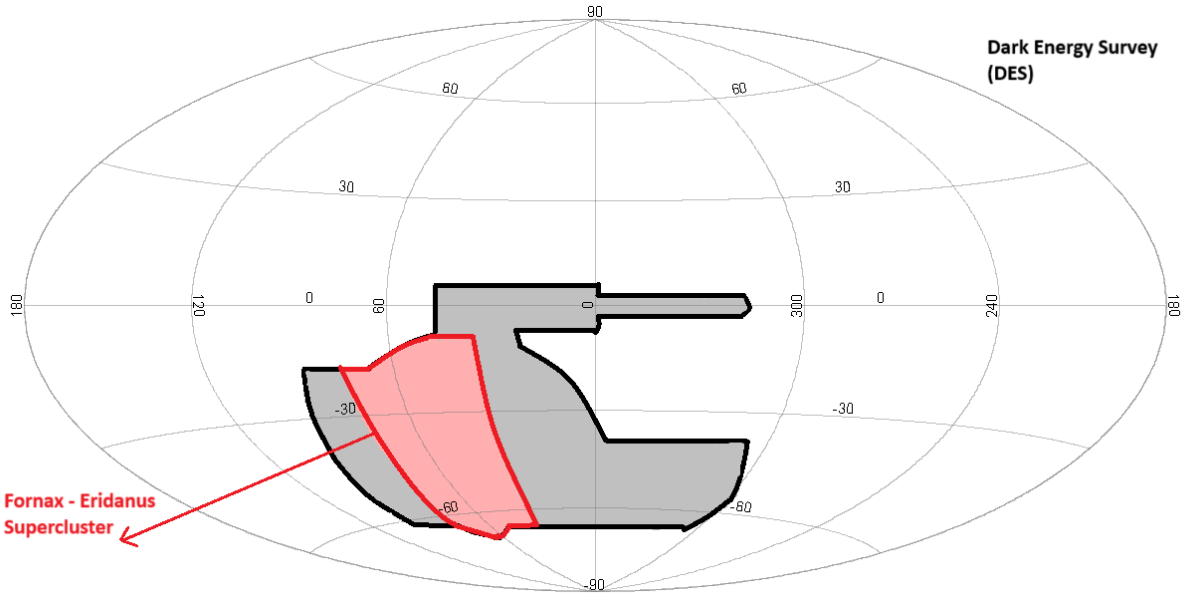

Figure 5: The footprint of the DES survey (black), the region of the Fornax-Eridanus Supercluster used in this thesis (red) on the aitoff projection of the equatorial coordinates.

The methods used by T21 to produce the LSB catalog are summarised briefly here. They first removed artifacts from the DES Y3 GOLD catalog using colors, effective radius, ellipticities and surface brightness obtained by `SourceExtractor` (Bertin and Arnouts 2010). The definition of LSBs adopted was from Greco et al. 2018 as $R_{e,g} > 2".5$ kpc[1] and $\bar{\mu}_e(g) > 24.2$ mag arcsec^{-2}. Additionally, a machine learning classification algorithm was used to remove contaminants from diffraction patterns, bright regions of Galactic cirrus, substructures of large spirals and tidal ejecta of high surface brightness galaxies. After visual inspection of these galaxies, galfitm was used to fit a single-component Sérsic function to galaxy radial profiles.

Some extended LSBs can also be massive (e.g., Bothun et al. 1985). However, due to the surface brightness-luminosity relation (Binggeli et al. 1984), most LSBs are dwarfs. In addition to this, the DES reduction pipeline is optimised for faint and small galaxies which can exclude detection of extended (and massive) LSB objects. As a result, the T21 catalog consists mainly of LSB dwarf

[1] At the mean distance of the Fornax Wall (20 Mpc h^{-1}), 1 arcsec $\approx$ 0.1 kpc

galaxies[2]. Some examples of LSBs in the T21 catalog are shown in Figure 6.

The selections by T21 was tailored to remove massive galaxies and most of the artifacts. However, on inspection of a sample (also described in Section 3.1.4), we found that some massive galaxies passed their selections. Their sample is also estimated to include LSBs upto a distance of 100 Mpc (T21), which is farther than the Fornax-Eridanus supercluster. Due to the above reasons, it is required to identify LSBs in the T21 catalog that are members of the Fornax-Eridanus supercluster.

Figure 6: Some early-type (left) and late-type (right) LSBs in the T21 catalog.

[2]In the SDSS band, dwarfs have a r-band magnitude $M_r > -19$ mag; Choque-Challapa et al. 2021. The magnitudes obtained in 3.1.6 and shown in 4.1.4 are in this range

3 Methods

In this chapter, we first define the environments within the supercluster. Then, we obtain the supercluster dwarf (SC dwarf) catalog from the T21 catalog by identifying members using scaling relations and known groups that are outside the Fornax Wall. Finally, we also calculate the absolute magnitudes and the stellar mass of the galaxies by adopting distances based on the groups in the Fornax Wall.

3.1 Regions of interest

In this section, we present a preliminary catalog of supercluster LSBs by first identifying galaxies located within the Fornax Wall. Then, we divide the population into two: group and pristine galaxies.

3.1.1 Galaxies within the 2D Fornax Wall

Filaments and walls usually have diameters ranging from 1 to 7 Mpc h^{-1} (Cautun et al. 2014). For the Fornax Wall, a radius of $r = 3$ Mpc h^{-1} was selected by R24, as it produced the highest density contrast between all the filament structures in their catalog and surrounding low density regions. Since this selection was based on the 3D locations of massive galaxies, we adopt the same radius for our analysis.

The T21 catalog encompasses a region significantly larger than the area within the radius of the Fornax Wall (see Figure 5 and 7). Given that the catalog uses equatorial coordinates, we use the angular separation of galaxies from the Fornax Wall spine as a proxy for the projected distance from the spine. We convert the radius $r = 3$ Mpc h^{-1} to degrees and find a radius of $\sim 9^{\circ}$. We adopt $r = 10^{\circ}$ in this thesis to include regions that may be excluded due to projection effect.

To identify LSBs within this radius, we use the `search_around_sky` function from Python's `astropy`. This function calculates the angular separation between objects in 2D spherical coordinates. Since the perpendicular distance of any point from a curve is also the shortest distance to the curve, we designate the minimum angular separation of a galaxy from the locus of the Fornax Wall spine as its projected distance.

3.1.2 Group and Pristine environment

As the properties of galaxies within groups and outside groups are known to be different, the LSBs are divided into two populations: all galaxies within one virial radius of groups and the Fornax cluster are "group galaxies" and the galaxies outside one virial radius of groups and the Fornax cluster are "pristine" galaxies.

The Fornax Wall has only one structure that is termed a "cluster", the Fornax cluster. In this text, we refer to all galaxies within one virial radius of both groups and the Fornax cluster as group galaxies. Additionally, the pristine environment includes galaxies that are in the outskirts of groups. These galaxies may be (partially) influenced by the cluster potential well and are therefore, not isolated galaxies.

Figure 7 illustrates the 20 groups and clusters that belongs to the Fornax Wall identified by R24 using the group catalog compiled by Tempel et al. 2016. We match the Fornax Wall Brightest Cluster Galaxies (BCGs) with the galaxy catalog by Kourkchi and Tully 2017 to find their corresponding

groups, the group centers and their projected virial radii R_v. For the cases with no estimated virial radius, a value of 1 deg is assumed. This is chosen based on the known virial radius of similar small groups which ranges from 0.6 to 1.3 deg. The compiled properties of the groups are listed in Table 1.

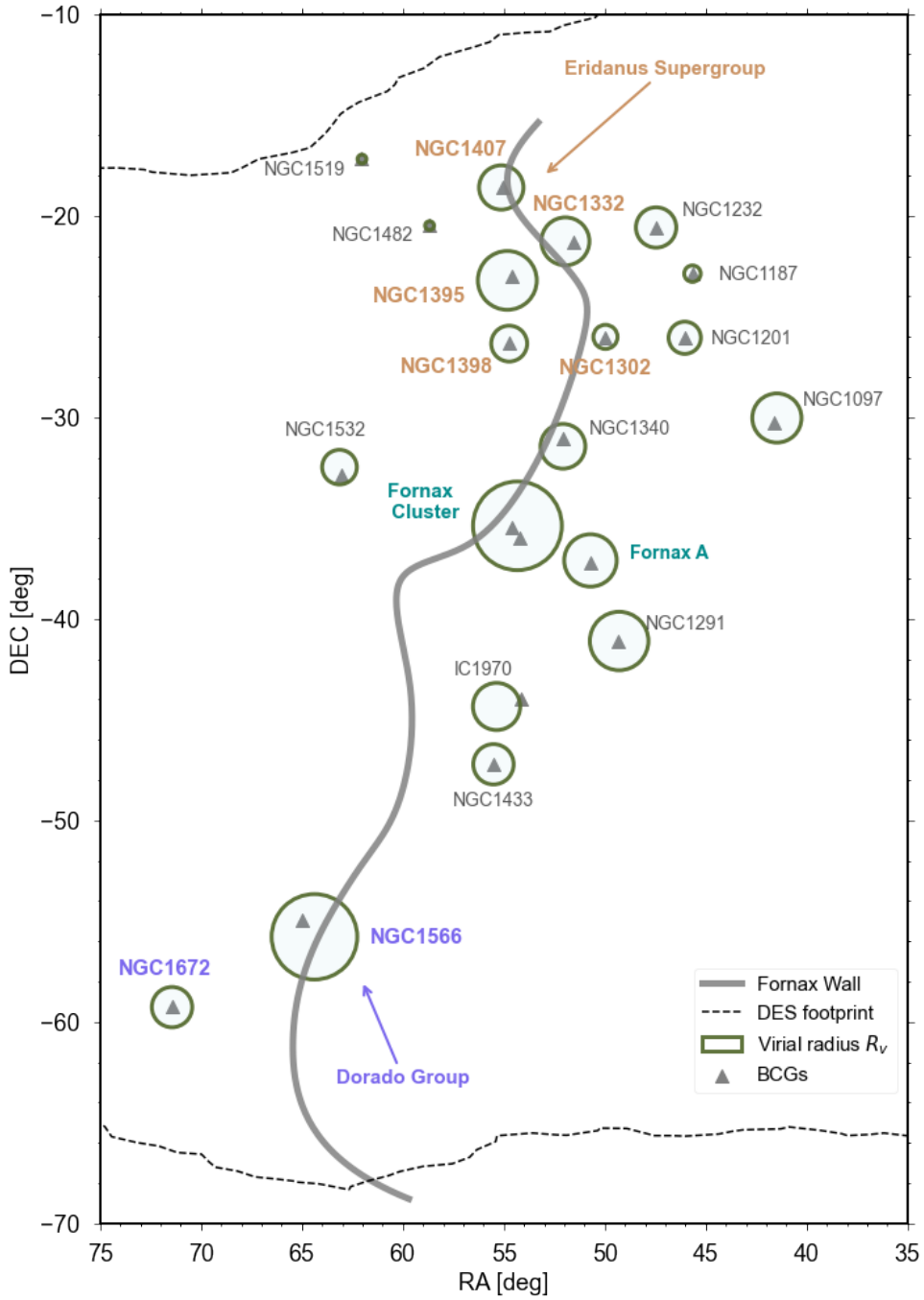

Figure 7: The Fornax Eridanus (FE) Supercluster: The gray line traces the 2D projection of the filaments that form the Fornax Wall spine (R24). Green circles and their corresponding labels represent the Fornax Wall groups (R24, Tempel et al. 2016) and their virial radii (Kourkchi and Tully 2017). Gray points are the brightest cluster galaxies (BCGs) in the groups. The Eridanus Supergroup, Fornax cluster and the Dorado group are highlighted with different colors. The dotted-line is the DES footprint, which encloses nearly all of the Fornax Wall.

The galaxies within 10° from the spine is then segregated into group and pristine galaxies using the `search_around_sky` algorithm described previously. The catalog obtained after this step is hereafter called the initial SC dwarf catalog, which is then used to remove background and foreground galaxies.

The initial SC dwarf catalog has a total of 5240 LSBs with 4443 of them in the pristine environment and 797 in groups.

Group ID	RAJ2000	DEJ2000	R_v [deg]	N_{LSB}	θ [deg]
Fornax	54.3184	-35.3897	2.2	260	0.83
Fornax A	50.7026	-37.1084	1.3	47	4.21
NGC1395	54.8196	-23.2141	1.46	75	2.48
NGC1332	51.9446	-21.2755	1.19	40	0.8
NGC1097	41.4692	-30.0411	1.22	32	9.1
NGC1532	63.1319	-32.4793	0.86	9	5.83
NGC1201	46.0326	-26.06	0.8	15	4.46
NGC1232	47.4509	-20.588	1.0	9	4.51
NGC1302	49.9607	-26.0177	0.6	11	0.96
NGC1340	52.0658	-31.4462	1.11	19	0.72
IC1970	55.3533	-44.3547	1.17	14	3.0
NGC1187	45.6511	-22.8797	0.41	2	5.0
NGC1519	62.0185	-17.1936	0.22	0	6.92
NGC1407	55.1204	-18.6044	1.1	91	0.31
NGC1398	54.7286	-26.3501	0.89	23	3.12
NGC1482	58.6702	-20.4947	0.22	0	4.02
NGC1291	49.2825	-41.1056	1.45	32	7.48
NGC1672	71.4255	-59.2699	1.0	8	3.12
NGC1566	64.3718	-55.7811	2.12	98	0.11
NGC1433	55.5065	-47.2222	1.0	12	2.86

Table 1: Column 1: Groups within 10° around the Fornax Wall spine. Column 2 and Column 3: Equatorial coordinates of the group center. Column 4: Projected virial radius in degrees from Kourkchi and Tully 2017. Column 5: Number of LSBs in the initial SC dwarf catalog within one virial radius. Column 6: Distance of each group from the Fornax Wall.

3.1.3 Membership: Color-magnitude diagram

Previous studies on dwarf galaxies use scaling relations to remove background galaxies and identify cluster members (e.g., Venhola et al. 2018). We justify the usage of these scaling relations to identify the Fornax Wall group and pristine galaxies in this section.

In the color-magnitude (CM) space, early-type bright galaxies in clusters form a linear relationship with a nearly flat, negative slope called the red-sequence. Figure 8 shows the red sequence formed by Coma cluster members below $M_H < 15$ mag. Background galaxies are redshifted. Some appear below the red-sequence if they are very blue while most appear above the red-sequence with lower

luminosity. A large number of these background bright galaxies were removed by T21 due to their selection criteria mentioned in Chapter 2. In addition to this, they also explicitly removed galaxies with $g - i > 1.4$ mag.

Some low-luminosity cluster members are known to lie above the red sequence as outliers which is also seen in Figure 8. Compact dwarfs that were formed from larger galaxies are a possible outlier (e.g., Price et al. 2009, Hamraz et al. 2019). As they are thought to be formed by stripping of the outer parts of a galaxy, generally, they have $R_e(B) < 0.2$ kpc and surface brightness higher than LSBs (Price et al. 2009). The selections made by T21 have already excluded these galaxies. In addition to compact dwarfs, dusty galaxies can also appear above the main sequence. In general, LSBs are considered to have low amounts of dust as compared to brighter galaxies (see Hinz et al. 2007) due to their diffuse nature and relatively low star formation (Vallenari et al. 2005). However, there is some evidence that they can have a variety of dust levels (Junais et al. 2023, Liang et al. 2010). For example, early-type galaxies with blue centers have been observed in far-infrared wavelengths (De Looze et al. 2010). Although dust reddening is usually small for dEs in clusters (Hamraz et al. 2019), we do not have sufficient information on isolated LSBs. It is possible that star-forming LSBs found in isolated regions have dust content that makes them appear red. In previous dwarf galaxy studies like Venhola et al. 2018, background galaxies were considered to have $g - r$ and $g - i$ colors 3σ greater than the BCG instead of using the red sequence. This resulted in the inclusion of these outliers. To retain potential dusty LSBs in our catalog, we perform a similar selection.

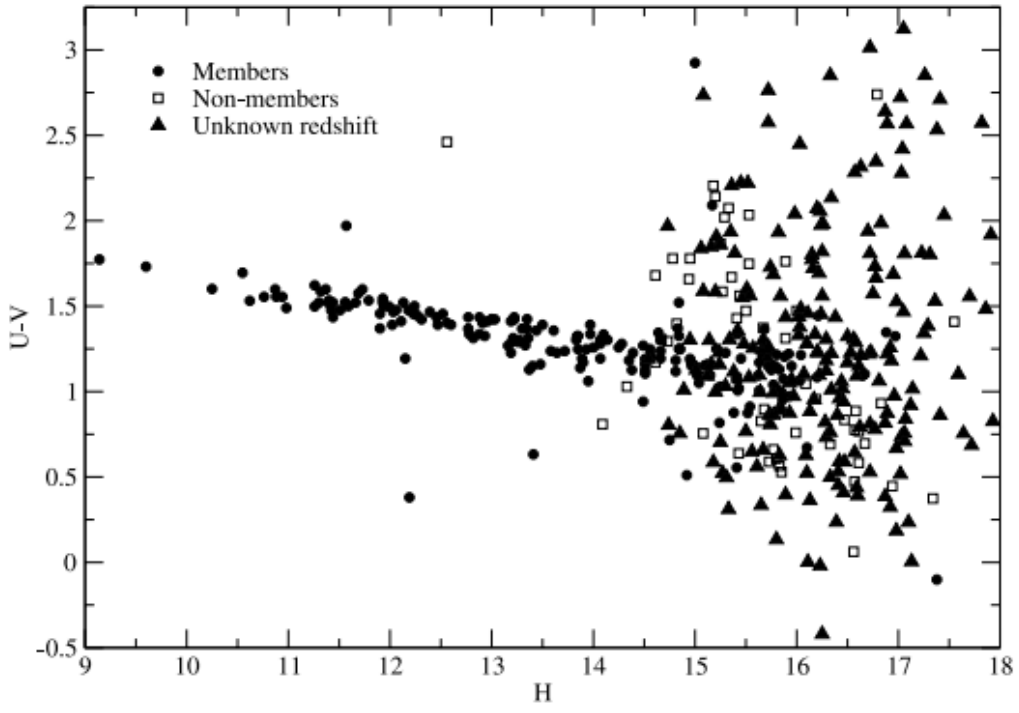

Figure 8: The color-magnitude diagram of galaxies in the central region of the Coma cluster adapted from Eisenhardt et al. 2007. The filled black circles represent cluster members. The squares represent non-member galaxies and the filled triangles are galaxies with unknown redshift.

The preferred method would be to use the BCGs belonging to each group. However, by searching the SIMBAD (Wenger et al. 2000) database, we found only the Johnson and Cousins magnitudes of the

Fornax Wall BCGs. These values can be converted to SDSS filter magnitudes using the equations in Jester et al. 2005. To obtain $g-r$ and $g-i$ colors, B, V, R and I magnitudes are required. Only 6 among the 20 BCGs had all four magnitudes. Figure 9 shows that the bright LSBs ($m_r < 19$ mag) lie along the red sequence formed by the Fornax dwarf galaxy catalog by Su et al. 2021 in both group and pristine environments. As the BCGs would lie along this red sequence, using the Fornax cluster BCG colors for the entire sample is a good approximation. We further justify this in Appendix A.

For the Fornax cluster, Venhola et al. 2018 defines cluster members as $g-r \leq 0.95$ mag and $g-i \leq 1.35$ mag based on NGC1399 galaxy. We remove galaxies outside this range (see Figures 9). To exclude foreground contamination, 19 pristine and 2 group galaxies that have $g-r \leq 0$ mag and $g-i \leq 0$ mag are also removed based on the range of colors in previous works on the Fornax cluster (Venhola et al. 2022, Su et al. 2021).

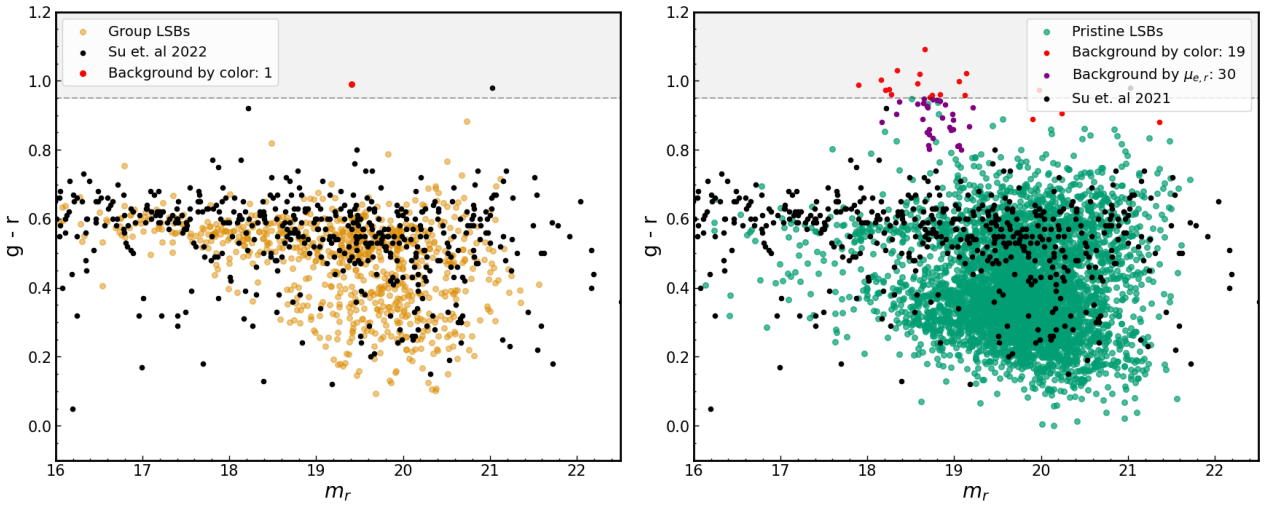

Figure 9: Color-magnitude diagram of Group LSBs (left; purple), (b) Pristine LSBs (right; orange). Background galaxies removed using color selection (red), using surface brightness-magnitude diagram (green) are included. The gray shaded region is the region removed by the $g-r$ color selection. Fornax cluster dwarf galaxies from Su et al. 2021 are plotted to highlight the red-sequence (black).

3.1.4 Membership: Surface brightness-magnitude diagram

The measured surface brightness of a galaxy does not change with distance because both the flux and the angular size follows the inverse-square law. Therefore, background bright galaxies appear as outliers on the surface brightness-magnitude diagram with fainter magnitudes and higher surface brightness. As done in Venhola et al. 2018, the sigma-clipped group and pristine surface brightness-magnitude relation is fit with a linear relation (Figure 10). Galaxies that are 3σ from the fit towards higher surface brightness would be considered background. However, there were no galaxies above this line in both cases due to the removal of high surface brightness galaxies in the g-band by T21. In the pristine environment, a clump of galaxies that were in the range of $0.8 < g-r < 0.9$ mag with $m_r < 19.5$ mag and $\bar{\mu}_{e,r} < 23.3$ mag arcsec^{-2} was found as outliers from the general trend (Figure 10). After visual inspection of this clump, 30 pristine galaxies were removed as they were bright ellipticals and background spirals galaxies.

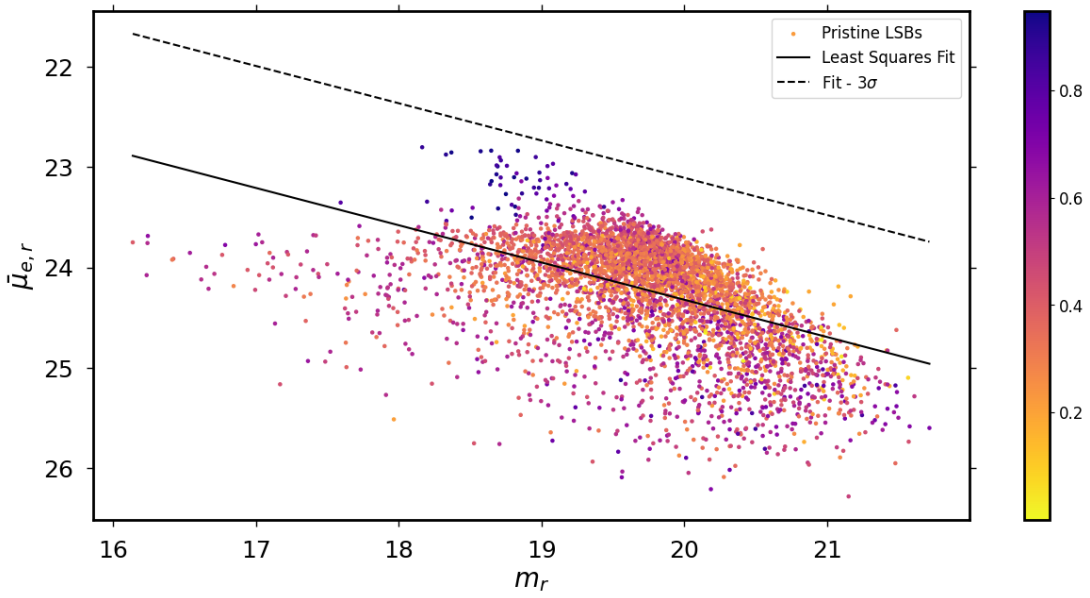

Figure 10: Surface brightness-magnitude diagram of pristine LSBs with $g-r$ color in the colorbar. The linear least squares fit of the diagram is included as the black line. The dotted line is 3σ away from the fit towards high surface brightness.

3.1.5 Membership: Removal of foreground and background groups

After the removal of background galaxies through scaling relations, the 2D distribution of the LSBs showed clumping that were not part of the Fornax Wall groups listed in Table 1. To investigate this, we overlay the group catalog by Tempel et al. 2016 and find that some of the clumping coincide with background or foreground groups. We remove the LSBs within groups from Tempel et al. 2016 that have the following conditions:

1. Comoving distance $D < 15$ Mpc and $30 < D < 150$ Mpc.
2. At least 5 LSBs are present within 0.5 deg from group center.
3. Group centers are not within 2 times the virial radius of Fornax Wall groups.
4. Group centers are not within 1 deg from massive galaxies.

The 150 Mpc limit for the comoving distance in the first condition is used because the T21 catalog is estimated to contain LSBs upto $\sim$ 100 Mpc based on the association of density peaks in the LSB distribution with known clusters (T21). As small groups that are present within the Fornax Wall were not identified by T21, it is possible that the catalog extends farther than 100 Mpc. The second condition ensures that the LSBs actually form a group. The third and fourth condition are imposed because some groups are found to coincide with massive galaxies (from R24) in the Eridanus region and the LSBs near them are most likely supercluster members.

Figure 11 shows the background and foreground groups that pass the above conditions. In total, we remove 237 pristine LSBs within one R_{200} radius of these groups. In addition to this, 215 galaxies in $55 < \text{RA} < 75$ and $-20 < \text{DEC} < -10$ (red points in Figure 11) are removed manually using `TOPCAT`

(Taylor 2005) after visually inspecting the crowded region. The final SC dwarf catalog contains 3926 LSBs in the pristine region and 791 group LSBs.

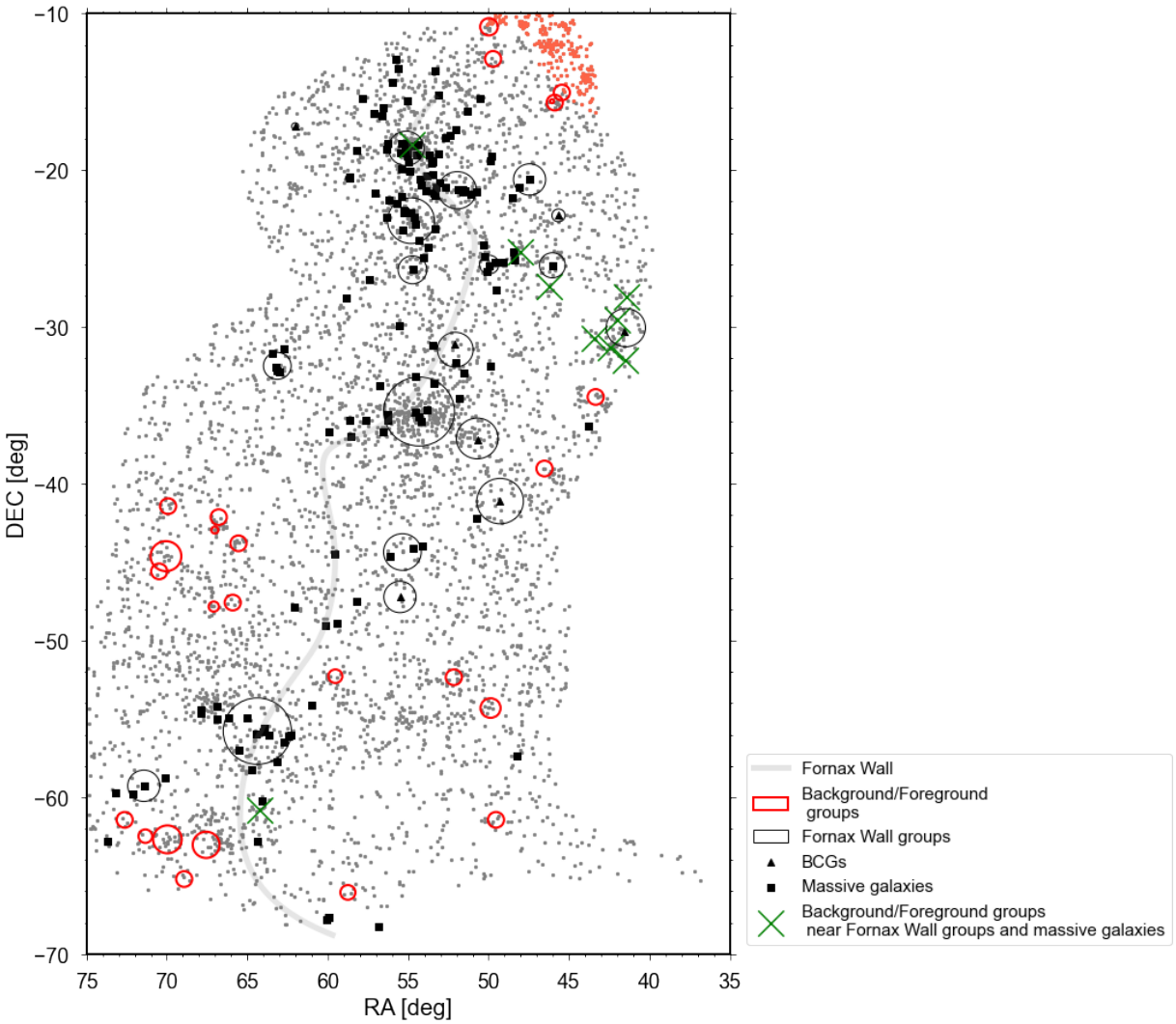

Figure 11: R_{200} radius of background and foreground groups within 15 - 30 Mp h^{-1} compiled from Tempel et al. 2016 (red circle). The background and foreground groups within 2 times the virial radius of Fornax Wall groups and 1 deg around massive galaxies (green cross). Area removed manually (red points), massive galaxies in the Fornax Wall from R24 (black points) and LSBs in the SC dwarf catalog after background removal through scaling relation (gray points) are also included.

3.1.6 Distances, Absolute Magnitudes and Stellar Mass

We calculate the absolute magnitude of the galaxies and their stellar mass in this section. To calculate the stellar mass M_*, we use the empirical relation produced by Taylor et al. 2011. They use the $g-i$ color and M_i as follows:

$$\log_{10}(\frac{M_*}{M_\odot}) = -0.68 + 0.70\,(g-i) - 0.4\,M_i. \quad (1)$$

The Fornax Wall has a distance range of 15 - 30 Mpc h^{-1}. Assuming all the galaxies are at its mean

distance of 20 Mpc h^{-1} can lead to absolute magnitudes that have errors of upto 1.5 mag. Another option is to use the nearest massive galaxy and adopt its distance. Figure 12 shows the distances of massive galaxies. They have a smooth variation in the bottom half of the Fornax Wall, but vary non-uniformly near the Fornax cluster and the Eridanus Supergroup regions in the 2D space. Using the nearest neighbour to adopt distances can thus introduce an additional bias due to projection effect. Therefore, a more robust approach is required.

In 3D, the Fornax Wall spine is positioned such that the Dorado group region is nearest and the Eridanus Supergroup region is the farthest from us (Figure 12). Taking advantage of this, we divide it into six segments as shown in the figure. We adopt the distances of the well-known groups in the segments. Segments 1, 2 and 3 are at a distance of 18.4 Mpc h^{-1} based on Dorado group's NGC1566. Segment 4 is at a distance of 20 Mpc h^{-1} based on the Fornax cluster. Segments 5 and 6 contain the Eridanus Supergroup and we use the distance of NGC1407 at 24 Mpc $h^{-}1$. We then calculate the absolute magnitude and stellar mass.[3]

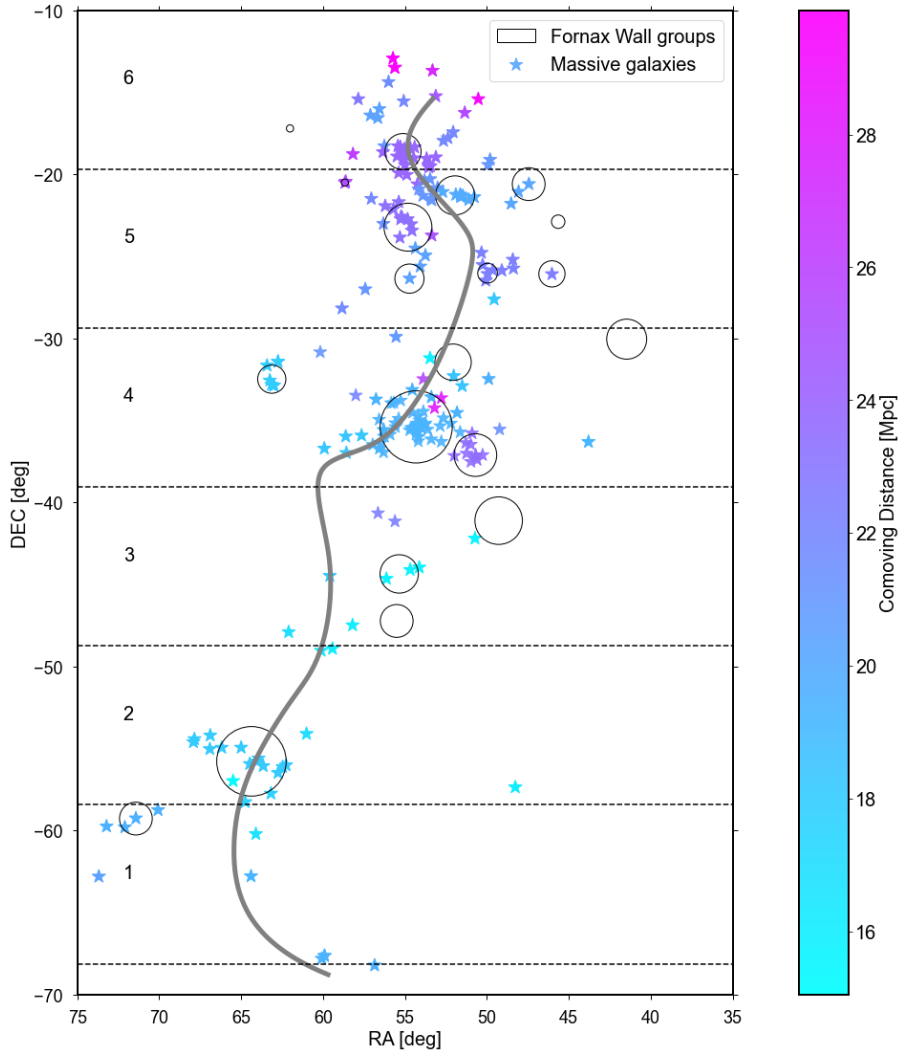

Figure 12: Massive galaxies in the Fornax Wall with their comoving distances from Tempel et al. 2016 in the colorbar. Black circles are the Fornax Wall groups. Dotted lines separate the Wall into segments which are labelled with numbers.

[3]For the conversion of effective radius from arcsec units to kpc, the distance of Fornax cluster 20 Mpc h^{-1} is used.

4 Results

In this chapter, we first discuss the properties of LSBs in the SC dwarf catalog obtained in Chapter 3. We investigate the morphology of the sample using the size-magnitude diagram, color-color diagram and the Sérsic index-magnitude diagram. We present the calculated absolute magnitudes and stellar mass. We then investigate the distribution of galaxies with respect to the Fornax Wall spine by using 2D density maps and calculating the fraction of galaxies with different properties as a function of distance from the spine. For each of these results, we compare galaxies in the group and pristine environment.

4.1 Properties of supercluster LSBs

In this section, we show the properties of the galaxies in the SC dwarf catalog to discuss their morphology and membership.

4.1.1 Size-magnitude relation

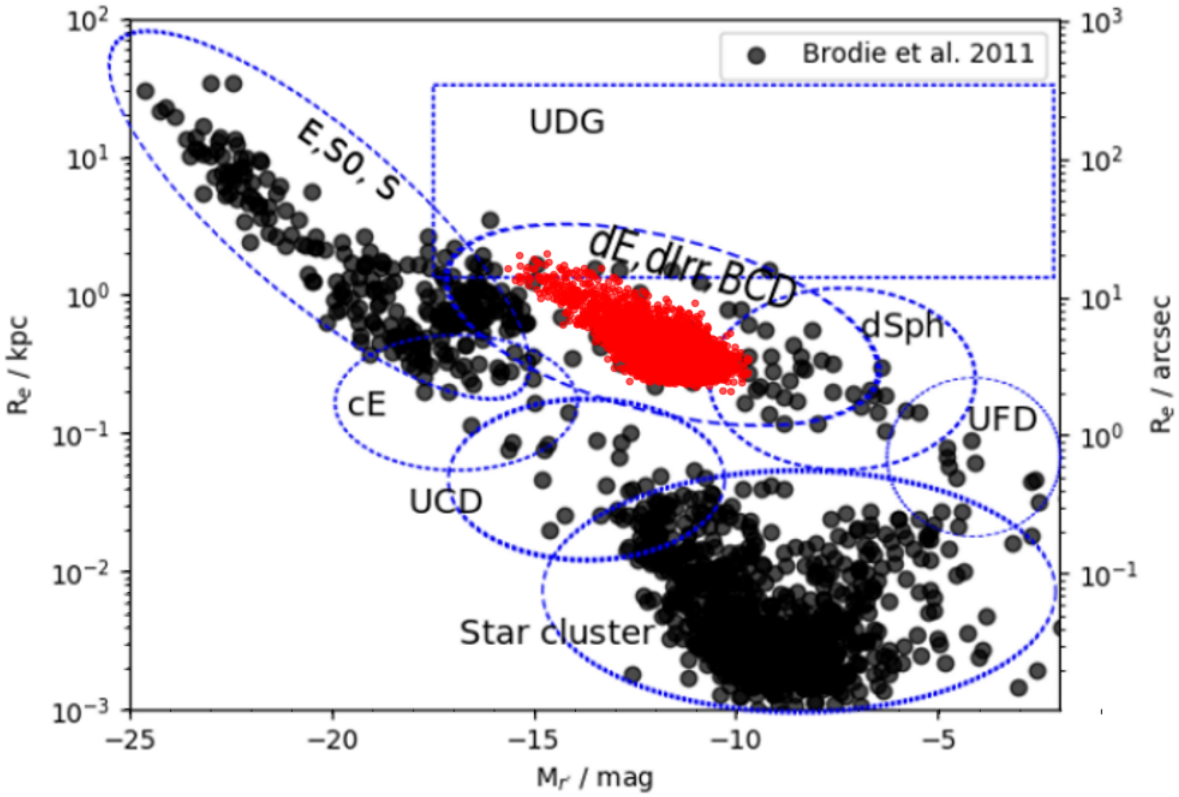

Figure 13: Effective radius $R_{e,r}$ vs absolute magnitude M_r diagram of LSBs (red points) overlaid on figure adapted from Venhola 2019 using the catalog by Brodie et al. 2011 (black points). The blue dotted ellipses denote the location of massive ellipticals (E), lenticulars (S0), spirals (S), dwarf elliptials (dE), dwarf irregulars (dIrr), blue compact dwarfs (BCD), dwarf sphericals (dSph), ultra-faint dwarfs (UFD), compact ellipticals (cE), ultra-compact dwarfs (UCD) and star clusters in the diagram.

The size($R_{e,r}$)-magnitude (M_r) relation can be used to hint at the morphology of galaxies. For example, bright, compact dwarf galaxies have a smaller magnitude and radius as compared to LSBs which are diffuse and larger. The relation is thus useful to identify contaminants in the catalog such as star clusters, massive galaxies or high surface brightness and compact dwarf galaxies. The blue ellipses and corresponding labels in Figure 13 depict the location of different objects in the size-magnitude diagram. The SC dwarf catalog is not contaminated by star clusters and giant galaxies, and galaxies in this catalog mostly lie within the ellipse labelled dEs, dIrrs and BCDs. The nucleus of BCDs have high surface brightness while their outer parts are faint. They may be part of the sample as they have effective surface brightness and magnitude similar to LSBs (Meyer et al. 2014). Dwarf sphericals (dSphs) are similar to dEs except that they are slightly redder and fainter (e.g., Seo and Ann 2023, Ann and Seo 2015). While these galaxies are thought to have different formation mechanisms, they constitute a small fraction of LSBs and distinguishing them is beyond the scope of this work.

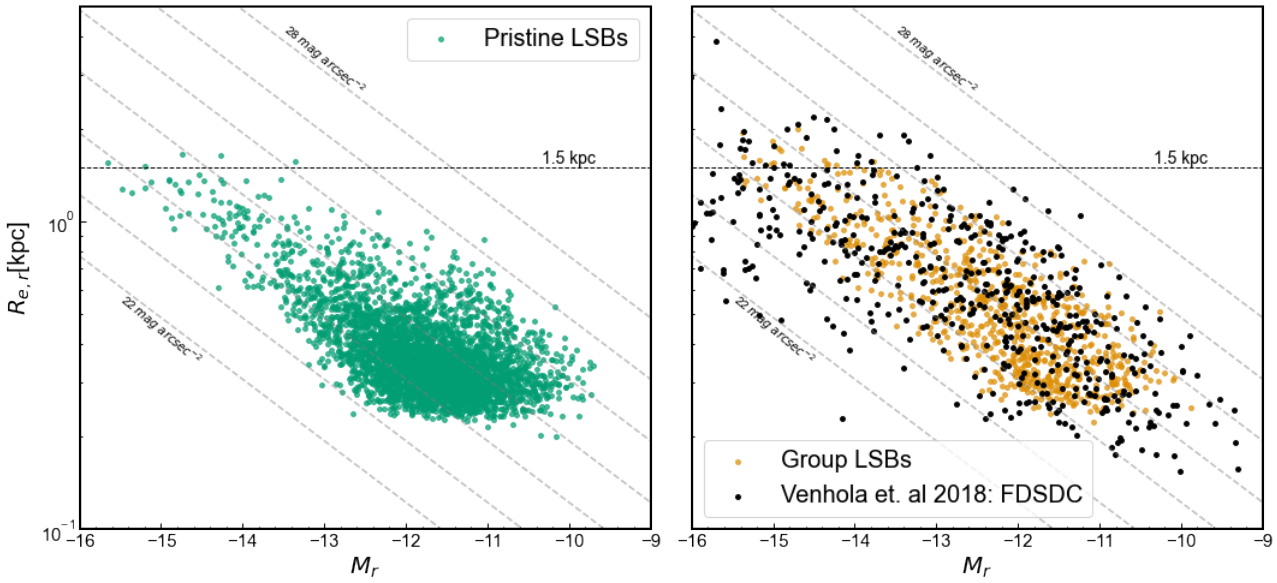

Figure 14: Size($R_{e,r}$)-magnitude(M_r) diagram for pristine LSBs (left) and group LSBs (right). The angled dashed lines represent the surface brightness values that correspond to each effective radius and magnitude. Above the horizontal black line (at 1.5 kpc) are ultra-diffuse galaxy candidates. The dwarf galaxies from FDSDC by Venhola et al. 2018 is also shown with the group LSBs (yellow squares).

The size-magnitude diagram for the group and the pristine galaxies in the SC dwarf catalog are shown in Figure 14. The group galaxies have six large LSBs with $1.65 < R_{e,r} < 2$ kpc that the pristine galaxies do not have. LSBs with $R_{e,r} > 1.5$ kpc are categorised as Ultra Diffuse Galaxies(UDGs) and are thought to have different formation mechanisms (refer Román and Trujillo 2017, Zaritsky et al. 2023). We find 5 UDG candidates in the pristine environment and 16 in the group environment.

We compare the group LSBs with the FDSDC dwarf galaxies. Approximately 45% of their catalog is in the SC dwarf catalog. Figure 14 shows that their catalog reaches depths upto $\bar{\mu}_{e,r}$ ∼28 mag arcsec^{-2} while the SC dwarf catalog reaches upto $\bar{\mu}_{e,r}$ ∼27 mag arcsec^{-2}. Some low luminosity LSBs with ($M_r >$ -10 mag) are also missing in our catalog. The FDSDC galaxies that have $\bar{\mu}_{e,r} > 23$ mag arcsec^{-2} are bright dwarfs and are not LSBs.

4.1.2 Color-color relation: Defining red and blue galaxies

In Figure 15, we show the color-color relation for the LSBs in the SC dwarf catalog. The histograms for $g-i$ and $g-r$ colors have two peaks, showing the bimodality in the color distribution. It has been well-established in the literature (e.g., Blanton et al. 2003) that red and blue galaxies form two distinct populations (peaks in the density of the points in Figure 15). In T21, galaxies with $g-i<0.6$ mag were defined as blue (late-type) and those with $g-i\geq 0.6$ mag were considered red (early-type). This segregation was defined using the intersection point of the Gaussian curves fit around each peak in the $g-i$ histogram. The black dotted line in Figure 15 represents the color definition ($g-i=0.6$ mag) used by T21. As this thesis uses parameters obtained in g and r band for analysis, we use $g-r$ values to define a galaxy's color. We fit the color-color diagram with a linear relation (slope $=0.65$, intercept $=0.06$). Finally, we define galaxies with $g-r>0.452$ mag as red and $g-r\leq 0.452$ mag as blue.

Figure 15 shows that blue LSBs dominate the SC dwarf catalog. T21 demonstrated that their catalog contains more blue LSBs than red LSBs, whereas other LSB catalogs, such as that of Greco et al. 2018, show equal populations of both. Whether blue LSBs dominate their sample due to their selection, error in photometry, impurity of the sample or if it represents an intrinsic distribution is unclear. It is important to note that this uncertainty may affect the conclusions drawn in this work.

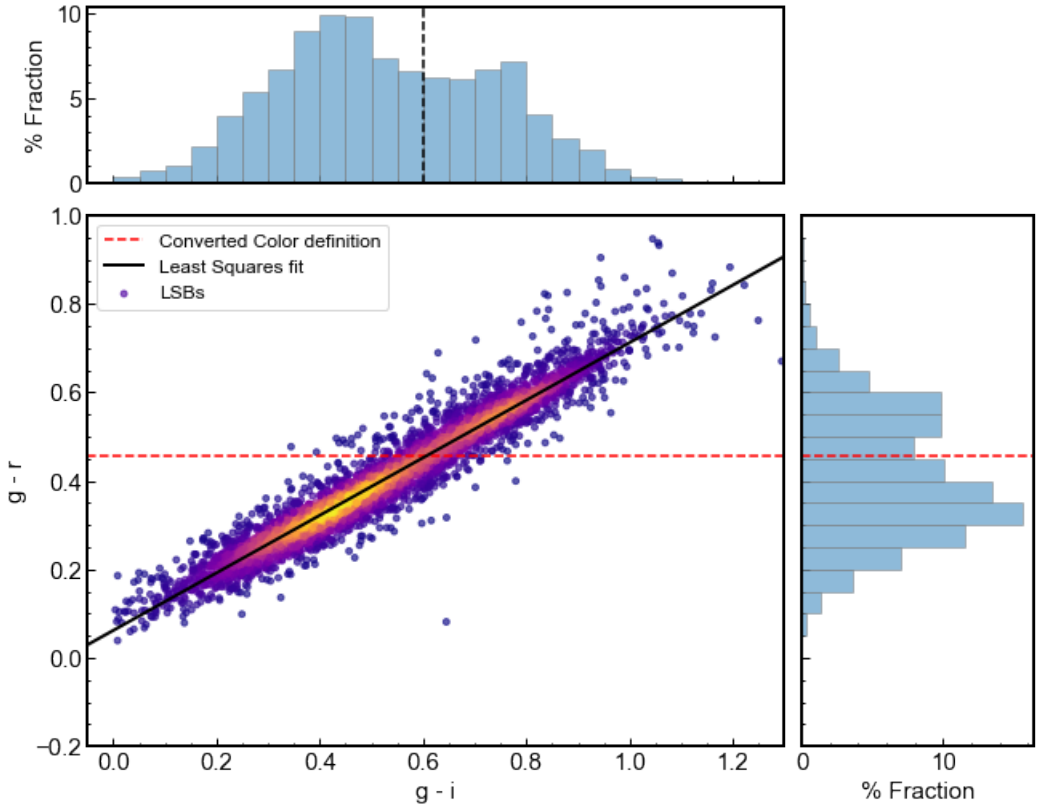

Figure 15: $g-r$ vs $g-i$ diagram of LSBs with the density of the scatter plot shown using colormap. The fit to the relation (black solid line) is included. The definition of galaxy color adopted by T21 (black dotted line; $g-i=0.6$ mag) and the corresponding value used in this thesis (red dotted line; $g-r=0.452$ mag) is included. The histograms show the fraction of galaxies in each axis.

4.1.3 Sersic index-magnitude relation

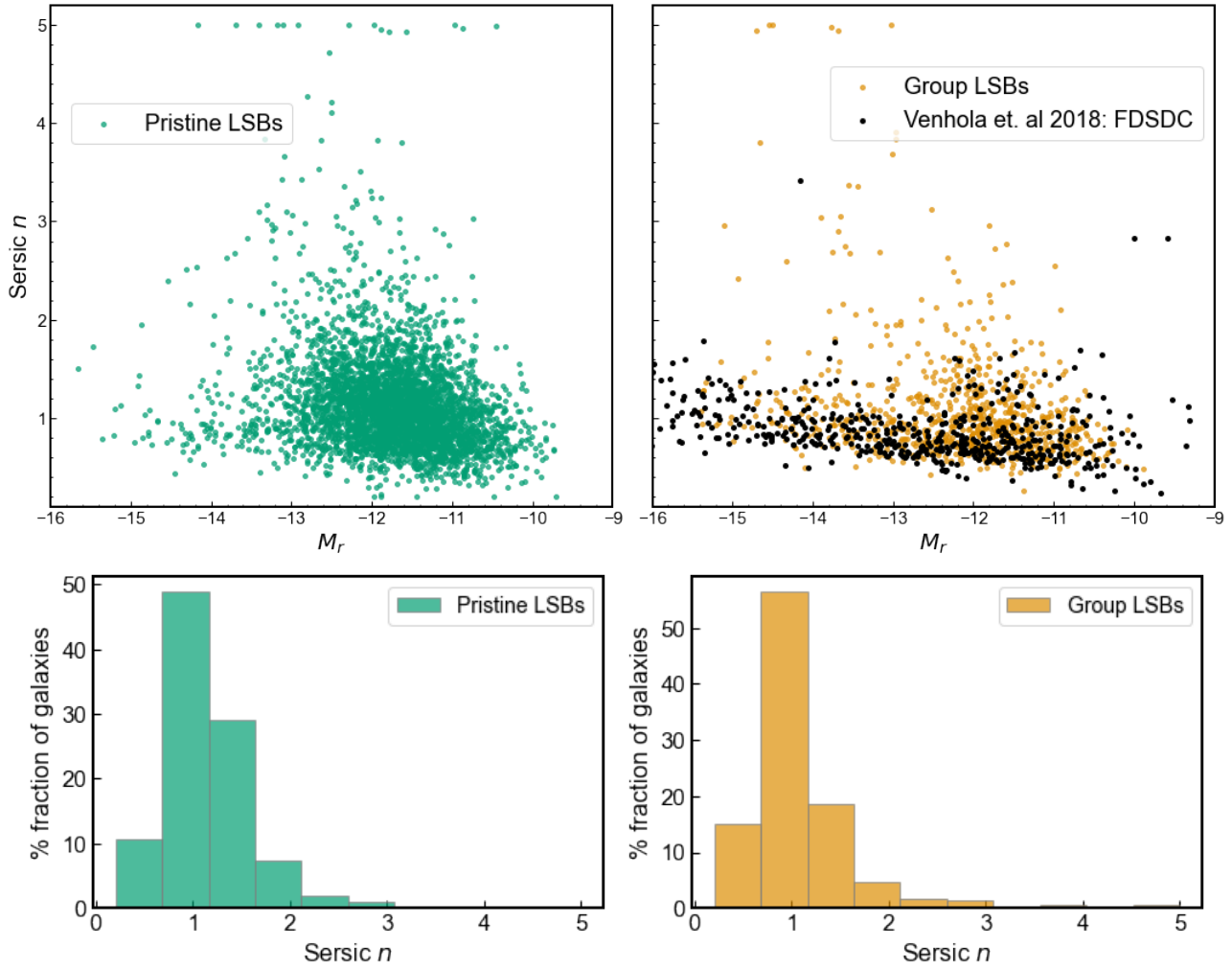

Figure 16: Sérsic n vs absolute magnitude M_r diagram of pristine (top-left) and group (top-right) LSBs. The dwarf galaxies from FDSDC by Venhola et al. 2018 is also shown with the group LSBs (black squares). The histogram of Sérsic n of pristine (bottom-left) and group (bottom-right) LSBs.

The Sérsic index n characterises the shape of a galaxy's radial intensity profile. An exponential profile similar to that of a galaxy disk corresponds to $n = 1$. Galaxies with a central concentration and a disk typically have higher n. In general, most LSBs are diffuse and do not have a distinct nucleus. Therefore, they typically have Sérsic $n \leq 1$ (e.g., Venhola et al. 2022). Venhola et al. 2022 showed that measurement uncertainties can cause scatter in the Sérsic index of faint galaxies, due to which the range of observed Sérsic index can extend up to $n = 2$. We find that the mean Sérsic n of pristine galaxies is 1.15 and the mean Sérsic n of group galaxies is 1.08.

Figure 16 shows the Sérsic index of pristine and group galaxies. The dwarf galaxies in FDSDC are mostly limited to $n < 2$ while the SC dwarf catalog has a large scatter, especially in the pristine environment. Galaxies within $2 < n < 4.5$ includes LSBs that are blue in color on visual inspection. It is likely that the photometry for these galaxies may not be accurate, however, it is possible that the blue LSBs in the pristine environment have a higher Sérsic index. Galaxies with $n \sim 5$ were mostly massive galaxies and some were Blue Compact Dwarfs (BCD). As galaxies with a distinct nucleus

and a disk require a double-component Sérsic fit while T21 uses a single-component Sérsic fit, the photometry of these galaxies are not reliable. The fraction of galaxies in the SC dwarf catalog with $n \geq 2$ is nearly zero (see histograms in Figure 16), therefore, this will not affect further analysis.

4.1.4 Magnitude and stellar mass function

The histograms of the calculated absolute magnitudes and stellar mass for galaxies in the SC dwarf catalog are shown in Figure 17. To check if the values agree with the literature, we use the FDSDC galaxies and compare the absolute magnitude M_r in our group catalog. The absence of SC group galaxies between $-16 < M_r < -18$ mag is due to the bright dwarf population in FDSDC, which does not comply with the LSB selection set by T21. The range of values in the SC dwarf catalog are within the range in FDSDC. The shape of the histogram is similar in both cases with increasing fraction of galaxies from the bright side to the peak at $M_r \sim -12$ mag after which incompleteness sets in.

Group and pristine galaxies show different distributions. Approximately 35% of group galaxies have $M_r < -12.5$ mag while only 15% of pristine galaxies are in this range. The fraction of group galaxies with $M_i < -13$ mag is 40% while the fraction of pristine galaxies is 18%. As the stellar mass is calculated using M_i, the distribution of stellar mass is similar to M_i. Nearly 47% of group galaxies have $\log M_* > 6.5\, M_\odot$ while 22% of pristine galaxies have $\log M_* > 6.5\, M_\odot$.

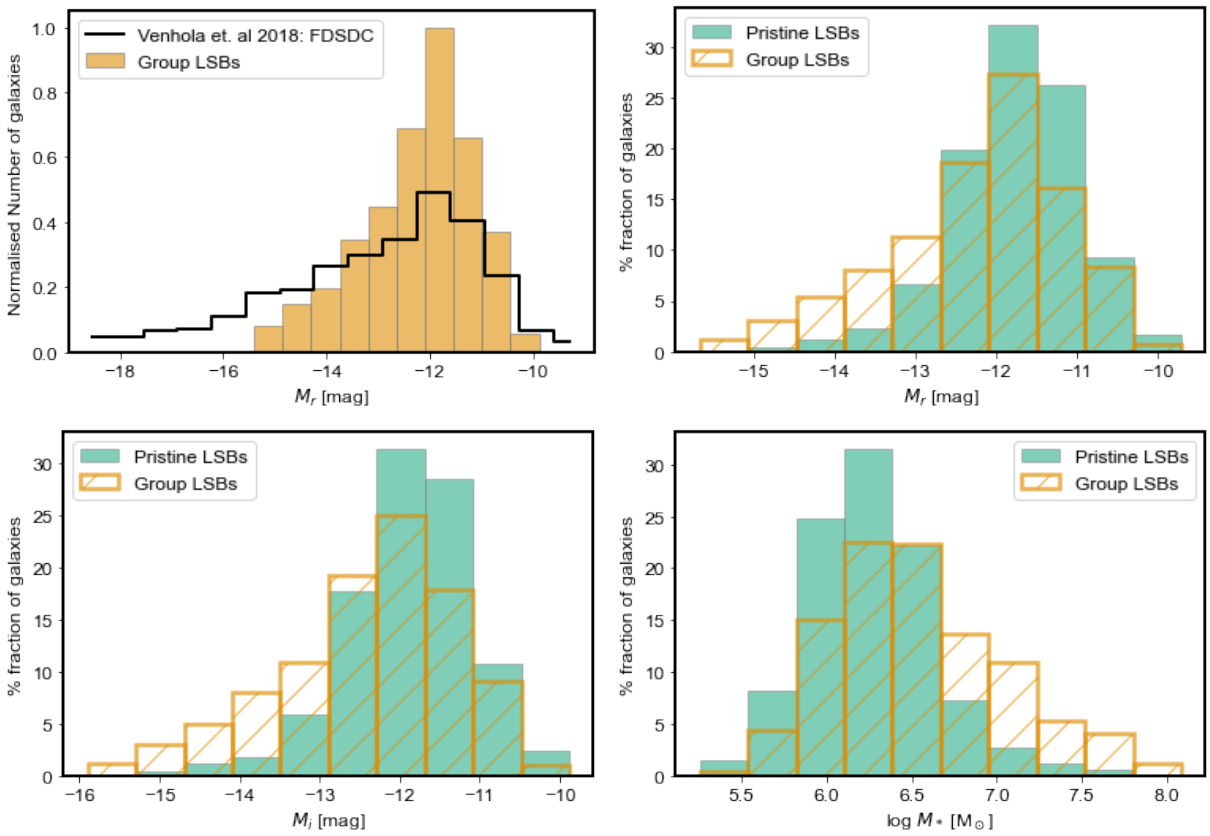

Figure 17: The M_r histogram for group galaxies along with the histogram of dwarf galaxies in FDSDC by Venhola et al. 2018 (top-left) and the histograms of M_r (top-right), M_i (bottom-left), M_* (bottom-right) for the group and pristine galaxies are shown.

4.2 Distribution of galaxies and their structural properties

We study the distribution of LSBs, probe their morphology-density relationship and structure with respect to their distance from the Fornax Wall.

4.2.1 The 2D distribution of galaxies

In this section, we describe the distribution of LSBs within the Fornax Wall. We use Kernel Density Estimation (KDE) in the 2D plane to obtain density contours. Our goal is to identify regions of high density within the supercluster. Therefore, a kernel of size $\sim 2 \times 2$ deg^2 is used based on the virial radius of the Fornax cluster (2.2 deg). The densities are evaluated using `scipy.stats.gaussian_kde` on a grid spanning $-70 < DEC < -10$ along and $35 < RA < 75$. While KDEs produce a continuous distribution map, the estimated densities can spill over from high density regions to nearby areas. Therefore, it is important to look at the KDE in combination with the 2D distribution of LSBs, inorder to form conclusions.

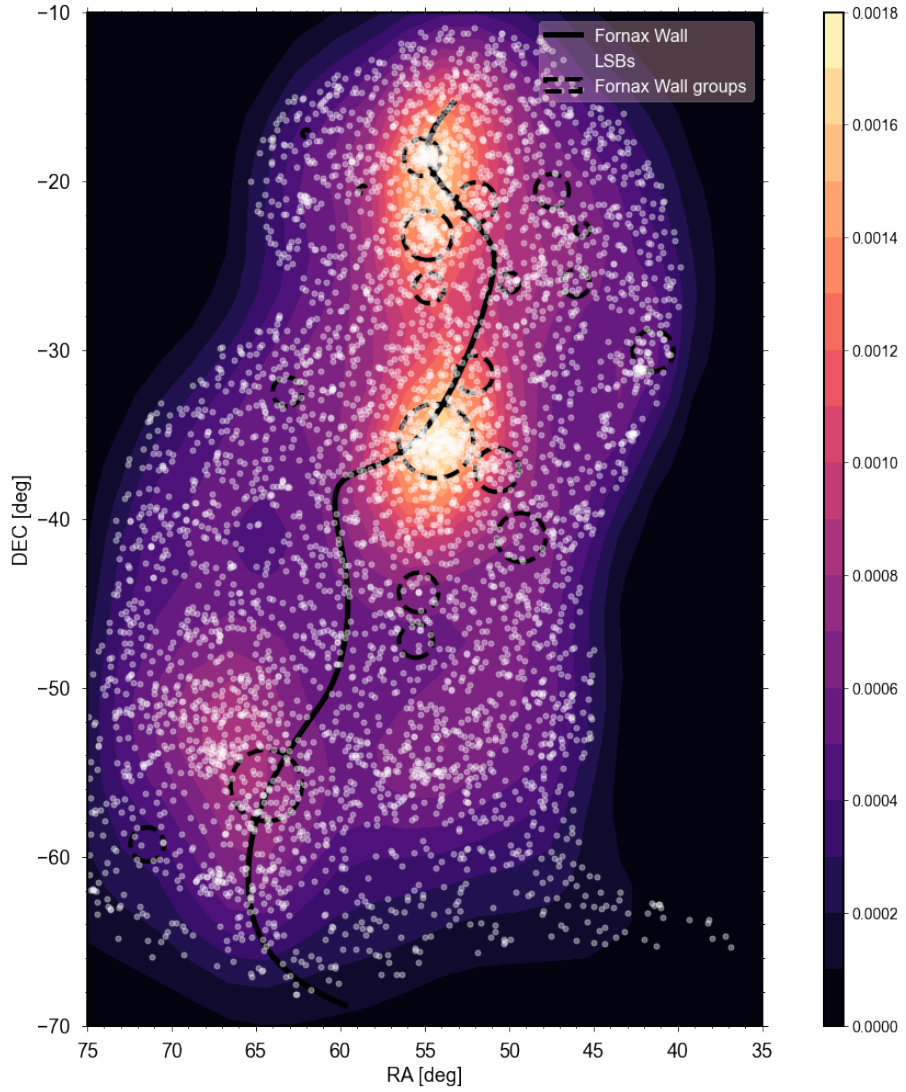

Figure 18: KDE for the spatial distribution of LSBs within the Fornax Wall and their 2D distribution (white points). The Fornax Wall (gray line) spine is also shown alongwith its groups (black dashed-circles).

Figure 18 shows the distribution of all LSBs that are part of the Fornax Wall. The galaxies are seen to be clumped in groups closer to the spine, mainly in the Eridanus Supergroup (over-density at the top) and the Fornax cluster region (over-density at the center). We also observe clumping near NGC 1566 of the Dorado Group (over-density at the bottom). Due to the well known morphology-density relation, most of the galaxies in the high density regions are expected to be early-type and red in color. T21 also found that red LSBs were clustered while blue LSBs were distributed uniformly. To identify if this is the case and if it depends on the proximity to the spine, we show the KDE for blue and red LSBs separately in Figure 19.

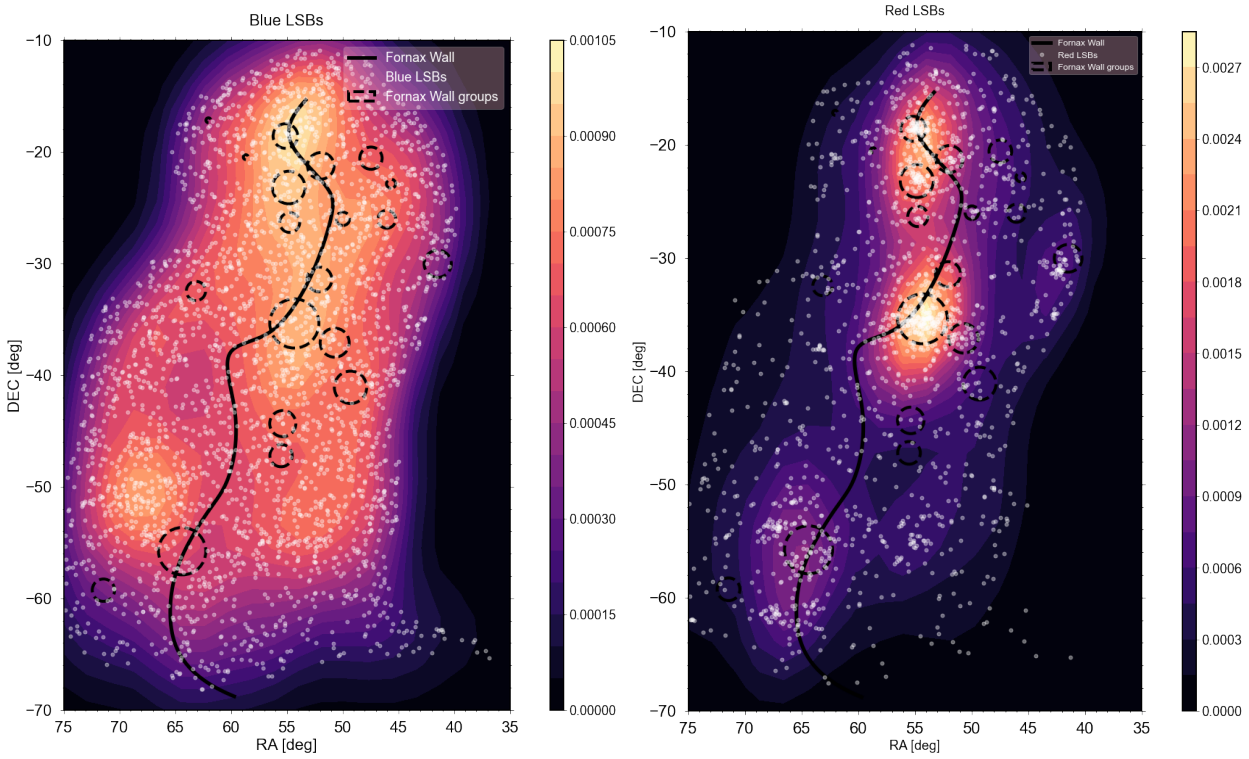

Figure 19: KDE for the spatial distribution of blue (left) and red (right) LSBs within the Fornax Wall and their 2D distribution (white points). The Fornax Wall (gray line) spine is also shown alongwith its groups (black dashed-circles).

The blue LSBs are located both in group and pristine environment. Any absence of blue galaxies seen in certain regions (for example, (RA, DEC) $\sim$ (65, -40)) is due to the removal of galaxies within background or foreground groups in Section 3.1.5. In contrast, the red galaxies are clustered in groups closer to the spine and the density of red galaxies is extremely low in the pristine environment. Red galaxies are, therefore, the main contributors to the gradient observed in the distribution of all the galaxies as expected.

4.2.2 Morphology-density relation in the Fornax Wall

The fraction of LSBs as a function of their distance from the Fornax Wall spine is shown in Figure 20. There are 15 % more galaxies that are in the bin at 1 deg from the spine than that are at 7 deg from spine. Therefore, LSBs are preferentially located closer to the spine, which has been defined using massive galaxies.

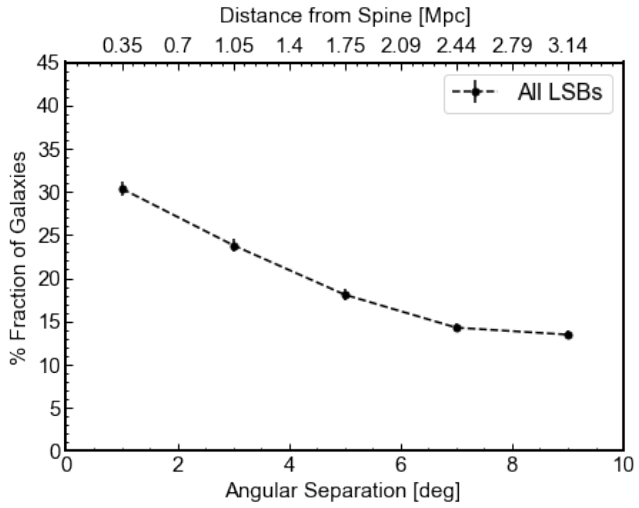

Figure 20: Fraction of galaxies in the SC dwarf catalog as a function of projected distances from the Fornax Wall spine. The distance bins are of size $\sim$ 2 deg as it is comparable to the size of the Fornax cluster. We assume a Poisson distribution in each bin to calculate their uncertainties.

To investigate the morphology-density relation, we plot the fraction of LSBs that are red and blue as a function of their distance from the spine in Figure 21. The fraction of red group galaxies decreases from $\sim$ 7% at 1 deg from the spine to nearly zero at 5 deg. Blue group galaxies exhibit a similar trend, with both fractions dropping to zero beyond 5 deg. However, at 1 deg, the fraction of red group galaxies is slightly ($\sim$ 4%) higher than that of blue group galaxies. At 3 deg, this difference diminishes, with fraction of red galaxies being only $<$1% more than blue ones. There are more early-type galaxies than late-type galaxies in groups within 3 deg from the spine while the groups farther than that have nearly equal populations of both morphology types.

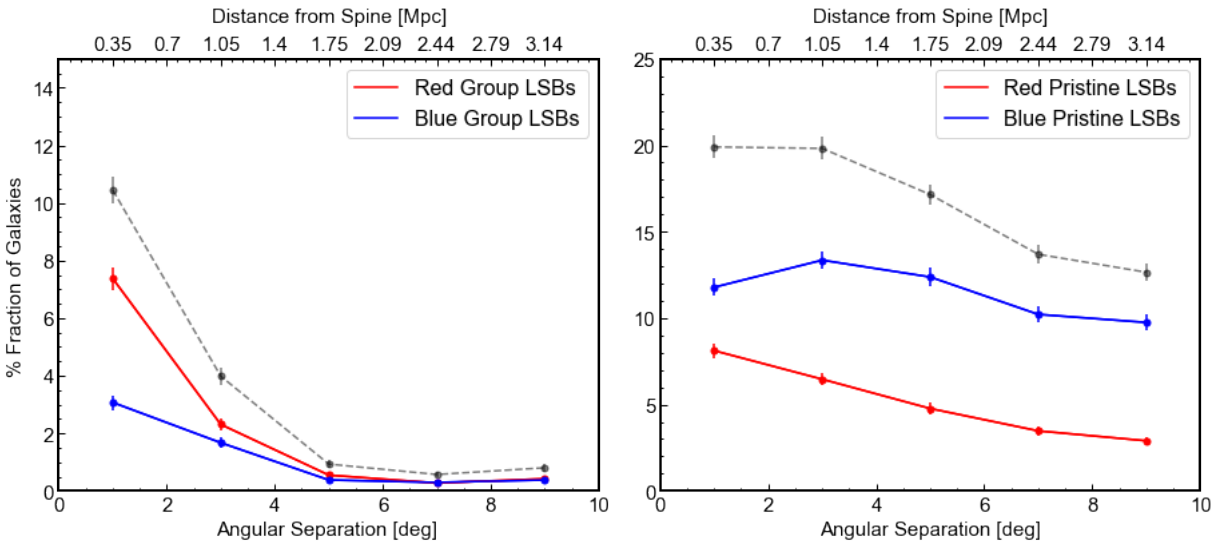

Figure 21: Fraction of the LSBs in the SC dwarf catalog that are red/blue in groups (left) and red/blue in the pristine environment (right) as a function of projected distance from the Fornax Wall spine. The dashed lines represent the fraction of LSBs that are both red and blue.

The trends of the red and blue pristine LSBs in Figure 21 are different from those in groups. A major difference is that the fraction of red galaxies is on average $\sim$ 5% smaller than the fraction of blue galaxies. This agrees with the 2D distribution in Figure 19 which showed that red galaxies are sparsely populated outside groups. While it is possible that a part of the blue galaxy population could

be due to background or foreground contamination, it is more likely that this difference is an intrinsic distribution as 70% of the pristine population are blue galaxies.

The red pristine galaxy fraction is smaller at 5 deg than at 1 deg similar to group galaxies. However, the slope is not as steep with only a 3% drop from 1 deg to 5 deg from the spine. We recall that the pristine galaxies do not necessarily contain only isolated galaxies. Groups can affect galaxies upto $\sim$ 3 times the virial radius from their centers (Cen et al. 2014). Some of the pristine galaxies may be part of the group or may be infalling galaxies that have been influenced by the group environment (Bahé et al. 2013). Previous studies show that infalling galaxies can undergo starbursts that may quench the galaxies before they enter a group (e.g., Mahajan et al. 2012). Therefore, the slightly higher fraction of red pristine galaxies closer to the spine might be due to the galaxies in the outskirts of Fornax cluster, Dorado group and the groups of Eridanus Supergroup.

4.2.3 Structural parameters of the LSBs

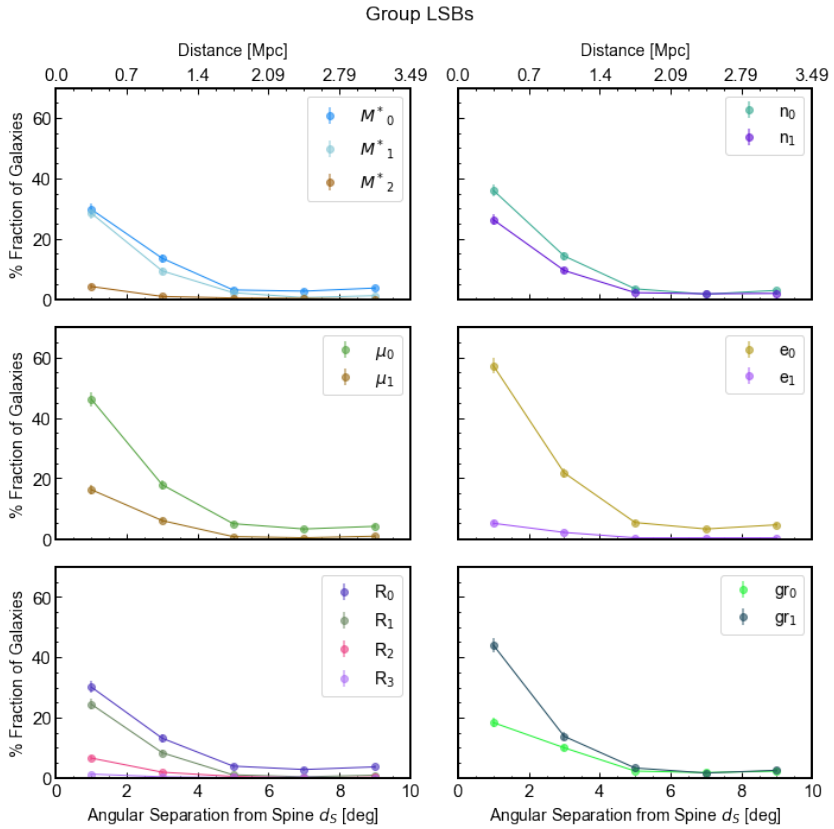

Label	Bin
μ_0	$\bar{\mu}_{e,r} < 25$ mag arcsec^{-2}
μ_1	$\bar{\mu}_{e,r} \geq 25$ mag arcsec^{-2}
M^*_0	log $M^* < 6.5\,M_\odot$
M^*_1	$6.5 \leq$ log $M^* < 7.5\,M_\odot$
M^*_2	log $M^* \geq 7.5\,M_\odot$
n_0	Sersic $n \leq 1$
n_1	Sersic $n > 1$
R_0	$R_{e,r} < 0.5$ kpc
R_1	$0.5 \leq R_{e,r} < 1$ kpc
R_2	$1 \leq R_{e,r} < 1.5$ kpc
R_3	$R_{e,r} \geq 1.5$ kpc
e_0	ellipticity < 0.5
e_1	ellipticity ≥ 0.5
gr_0	$g - r < 0.452$
gr_1	$g - r \geq 0.452$

Figure 22: Fraction of group LSBs as a function of projected distance from the Fornax Wall spine for M_*, Sersic n, $\bar{\mu}_{e,r}$, ellipticity, $R_{e,r}$, and $g-r$ color bins (left). Table with the labels in Column 1 and the corresponding bins in Column 2 (right).

In the previous section, we established that groups near the spine have more red galaxies than ones farther. We investigate if other galaxy properties show such a relation. The stellar mass M_*, effective surface brightness $\bar{\mu}_{e,r}$, effective radius $R_{e,r}$, Sérsic index n and the ellipticity have been divided into different bins provided in the table in Figure 22. The effective radius bin (R_4) contains the UDG candidates identified in Section 4.1.1. The two Sersic index bins each define flat and bulgy galaxies.

The $g-r$ bins retain the definitions in Section 4.1.2 for red and blue galaxies. The remaining bins have been defined by dividing the sample range into equal sizes.

The fraction of group LSBs for these bins is shown in Figure 22. Within 1 deg from spine, there are 55% more group galaxies with log $M_* < 7.5\ M_\odot$, 30% more galaxies with red color, 55% more galaxies with ellipticity < 0.5, 35% more galaxies with $\bar{\mu}_{e,r} < 25$ mag arcsec^{-1} and 35% more galaxies $R_{e,r} < 1$ kpc as compared to galaxies outside these ranges. Regardless of whether the population in the different bins mentioned above are the same galaxies or not, we speculate that there is some effect of the supercluster structure on group galaxies depending on their proximity to the spine.

The fraction of pristine LSBs is shown in Figure 23. All the properties have nearly constant fractions in every bin. Any difference in the fractions between each distance bin is $< 5\%$ for all the properties except for ellipticity, for which the difference is $< 10\%$. These trends are similar to those observed for $g-r$ color and suggests that there may be no environmental effect on pristine galaxies as a function of distance to the spine. We discuss the distribution of these properties in the next chapter.

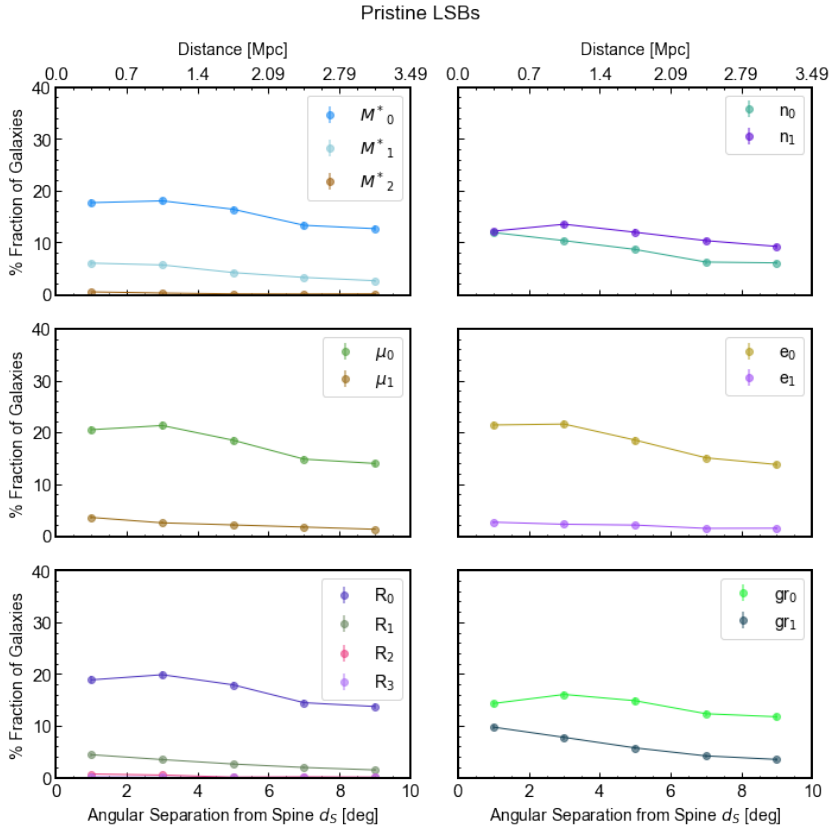

Label	Bin
μ_0	$\bar{\mu}_{e,r} < 25$ mag arcsec^{-2}
μ_1	$\bar{\mu}_{e,r} \geq 25$ mag arcsec^{-2}
M^*_0	log $M^* < 6.5\ M_\odot$
M^*_1	$6.5 \leq$ log $M^* < 7.5\ M_\odot$
M^*_2	log $M^* \geq 7.5\ M_\odot$
n_0	Sersic $n \leq 1$
n_1	Sersic $n > 1$
R_0	$R_{e,r} < 0.5$ kpc
R_1	$0.5 \leq R_{e,r} < 1$ kpc
R_2	$1 \leq R_{e,r} < 1.5$ kpc
R_3	$R_{e,r} \geq 1.5$ kpc
e_0	ellipticity < 0.5
e_1	ellipticity ≥ 0.5
gr_0	$g-r < 0.452$
gr_1	$g-r \geq 0.452$

Figure 23: Fraction of pristine LSBs as a function of projected distance from the Fornax Wall spine for M_*, Sersic n, $\bar{\mu}_{e,r}$, ellipticity, $R_{e,r}$, and $g-r$ color bins (left). Table with the labels in Column 1 and the corresponding bins in Column 2 (right). The table is the same as in Figure 22

5 Discussion and Conclusion

Matter flows in the Universe from low density regions such as voids to high density regions such as walls and filaments. It is likely that many galaxies within the Fornax Wall originated from nearby environments (R24). The variations in morphology across the different environments in the Fornax Wall may trace the evolutionary history of the supercluster (Einasto et al. 1980), similar to how the present structure of galaxies can reflect their dynamical history.

In the previous chapter, it was observed that LSBs in the Fornax Wall are clustered in groups that lie along the spine. As established by T21 (discussed in Section 1.5), this clustering is mainly observed in red LSBs while blue LSBs have a uniform distribution throughout the region. They attributed the clustering to known groups like the Fornax cluster. In our work, we observe that the clustering in red LSBs is mainly found in the large groups situated along the spine of the Fornax Wall. Groups farther from the Fornax Wall do not show significant clustering. This is in agreement with the morphological segregation observed by R24 for massive galaxies, who found that there were more early-type galaxies close to the spine. We also observed that the properties of group galaxies depend on the proximity to the spine.

Pristine galaxies showed no significant changes in its properties as a function of distance from the spine and ~ 30 % of pristine LSBs were found to be red. For LSBs, the efficiency of internal feedback is weak (Peng et al. 2010) and environmental processes are expected to dominate. As the pristine environment includes galaxies in the outskirts of one virial radius of groups, we suspect that a large population of these galaxies may be the precursors of pre-processed galaxies part of infalling groups.

In this chapter, we investigate group and pristine galaxies by converging on the population of LSBs that show signs of environmental impact and discuss this with respect to their location in the supercluster.

5.1 Environmental impact on LSBs

After investigating LSB distribution in the supercluster with color maps of properties listed in Section 4.2.3, we find that the effective radius of galaxies in and around groups is generally higher than in the pristine environment as seen in Figure 24. Figure 24 also shows the distribution of red and blue LSBs with $R_{e,r}$ in the colormap. Like with the clustering of galaxies observed by T21, red galaxies are the main contributors for the difference in $R_{e,r}$ between group and pristine environments, while blue galaxies have a similar distribution.

Figure 25 shows the Kormendy relation for the group and pristine LSBs that are red and blue. The histograms of the effective radius and effective surface brightness are fit with a skew normal distribution. In the case of effective radius, the two histograms intersect at 0.47 kpc beyond which the fraction of red pristine galaxies reduces to zero while the fraction of red group galaxies remains significant for all effective radius.

We investigate if the skew in the $R_{e,r}$ distribution of red pristine LSBs towards low $R_{e,r}$ may be due to background galaxies. The red LSBs with $\bar{\mu}_{e,r} > 23.5$ mag arcsec^{-2} have surface brightness and $g-r$ (colormap in Figure 25) equivalent to the rest of the population. Based on visual inspection, the red galaxies with $\bar{\mu}_{e,r} < 23.5$ mag arcsec^{-2} had a bright nucleus suggesting that they may be background galaxies. However, their fraction is nearly zero and they will not affect our analysis significantly. Thus, it is likely that the distribution observed is not severely affected by background galaxies.

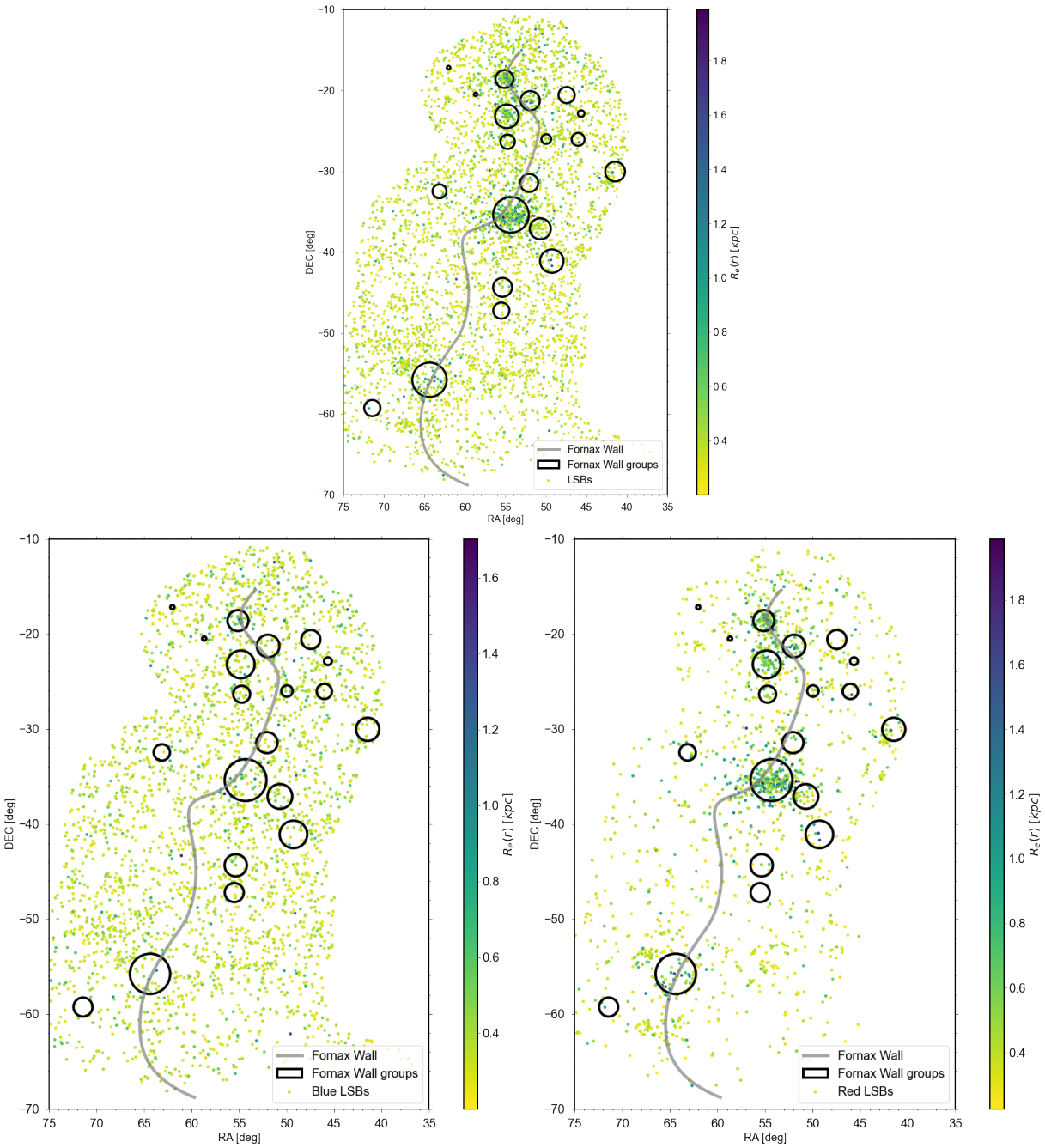

Figure 24: All the LSBs (top), blue LSBs (bottom-left) and red LSBs (bottom-right) in the 2D space with $R_{e,r}$ colormap. The Fornax Wall spine (gray line) and the Fornax Wall groups (black circles) are shown.

Nearly 66% of the red galaxies in groups have large radius ($R_{e,r} \geq 0.47$ kpc)[4] while only $\sim$ 30% of pristine have a large radius. In particular, the fraction of the pristine LSBs with the largest $R_{e,r}$ is nearly zero. Thus, red, early-type LSBs are significantly different in their size depending on their environment. This distinction is not seen in blue galaxies where both group and pristine environments have similar distributions for effective radius in Figure 25. In the case of effective surface brightness, there are $\sim$ 10% more red group galaxies and $\sim$ 10% more blue group galaxies with $\bar{\mu}_{e,r} > 24.24$ mag arcsec^{-1} than in the pristine environment. However, the peak of the blue group and pristine galaxy

[4]We expect that this value will change if the membership of the galaxies in the SC dwarf catalog is further refined

histograms are not different.

T21 found that large ($R_{e,g} > 0.6$ kpc) and faint ($\bar{\mu}_{e,g} > 26$ mag arcsec^{-2}) LSBs within the DES footprint were almost exclusively red. We find that $\sim 72\%$ of the LSBs in this range are red. As red galaxies are clustered in groups and since the $R_{e,r}$ and $\bar{\mu}_{e,r}$ distribution found in the Fornax Wall groups and the pristine environment are different, their finding may be due to an influence of the environment in groups. We further investigate the small LSBs ($R_{e,r} < 0.47$ kpc) and large LSBs ($R_{e,r} \geq 0.47$ kpc) separately as the differences in effective radius of the two environments is more prominent compared to the differences in surface brightness.

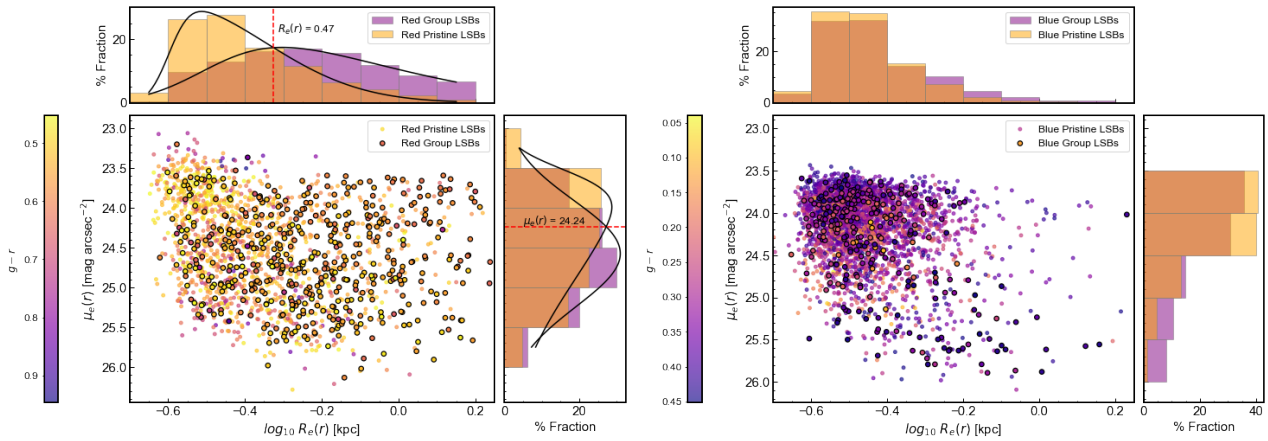

Figure 25: The Kormendy Relation ($R_{e,r}$ vs $\bar{\mu}_{e,r}$) of red (top) and blue (bottom) LSBs in the group and pristine environment with their $g-r$ color in the colormap. A skew normal function is fit to the histograms of red LSBs. The red dashed line corresponds to the intersection point of the red pristine and group histogram functions.

Large red LSBs are found only in groups or next to large groups close to the Fornax Wall in Figure 26. These regions also have multiple massive galaxies[5]. When compared to the distribution of small LSBs, they sparsely populate low density regions which suggests that their size might be due to interactions in high density regions.

The increase in size of LSBs in groups may be related to UDG formation. The mechanism that forms the large radius ($R_{e,r} > 1.5$ kpc) of UDGs has been debated in literature. Some suggest that they form through internal mechanisms. For example, in high spin dark matter halos that prevent gas from collapsing into a dense structure (e.g., Amorisco and Loeb 2016), or through outflows due to stellar feedback from starbursts at early epochs (e.g., Di Cintio et al. 2017). Meanwhile, others suggest that they are formed through environmental influence. For example, failed galaxies that are quenched by ram pressure stripping and tidal interactions before they reach high surface brightness (e.g., van Dokkum et al. 2015, Martin et al. 2019), tidal interactions with massive hosts (e.g., Jones et al. 2021), tidal forces in a cluster experienced during/after infall (e.g., Sales et al. 2020) or formation of diffuse galaxies from tidal debris created by interacting massive galaxies (e.g., Román et al. 2021). UDGs have been observed both in field (e.g., Leisman et al. 2017, Román et al. 2019) and in dense regions (e.g., Iodice et al. 2020, For et al. 2023). Their presence in the field suggests that large, diffuse galaxies can be formed without environmental influence but their distribution is not clear due to the difficulty in observing them.

In our work, we find that the largest LSBs are found only in groups close to the Fornax Wall. Many of

[5] A more robust analysis is required to confirm this for those that our outside groups.

the formation models listed above predict that diffuse and large galaxies can be found in low density regions. Only a few suggest that they are more likely to be found in groups (e.g., van Dokkum et al. 2015, Martin et al. 2019). Investigating the formation of large LSBs in the Fornax Wall may help resolve the formation mechanism of UDGs.

Based on UDG formation models, Jackson et al. 2021 studied LSBs using a cosmological simulation (NewHorizon). They suggest that LSBs form through a combination of supernova-driven gas outflows, tidal interactions and ram-pressure stripping. In their work, LSBs with lower surface brightness (accompanied by an increase in effective radius[6]) at a given stellar mass are formed from galaxies that were part of high density environment at early epochs. At high redshifts, their progenitors had faster gas accretion which increased star formation and thus, the strength of supernova-driven feedback. The gas outflows due to feedback decreased their surface brightness and increased the effective radius as both gas and old stellar population were pushed out. Both ram pressure stripping and tidal interactions can trigger star formation which then triggers gas outflows. Tidal interactions can also heat up the matter in galaxies, increasing their effective radius. Furthermore, progenitors of LSBs with "high" surface brightness at a given stellar mass were found in low density environments and did not have strong outflows. Their effective radius grew much slower resulting in smaller galaxies.

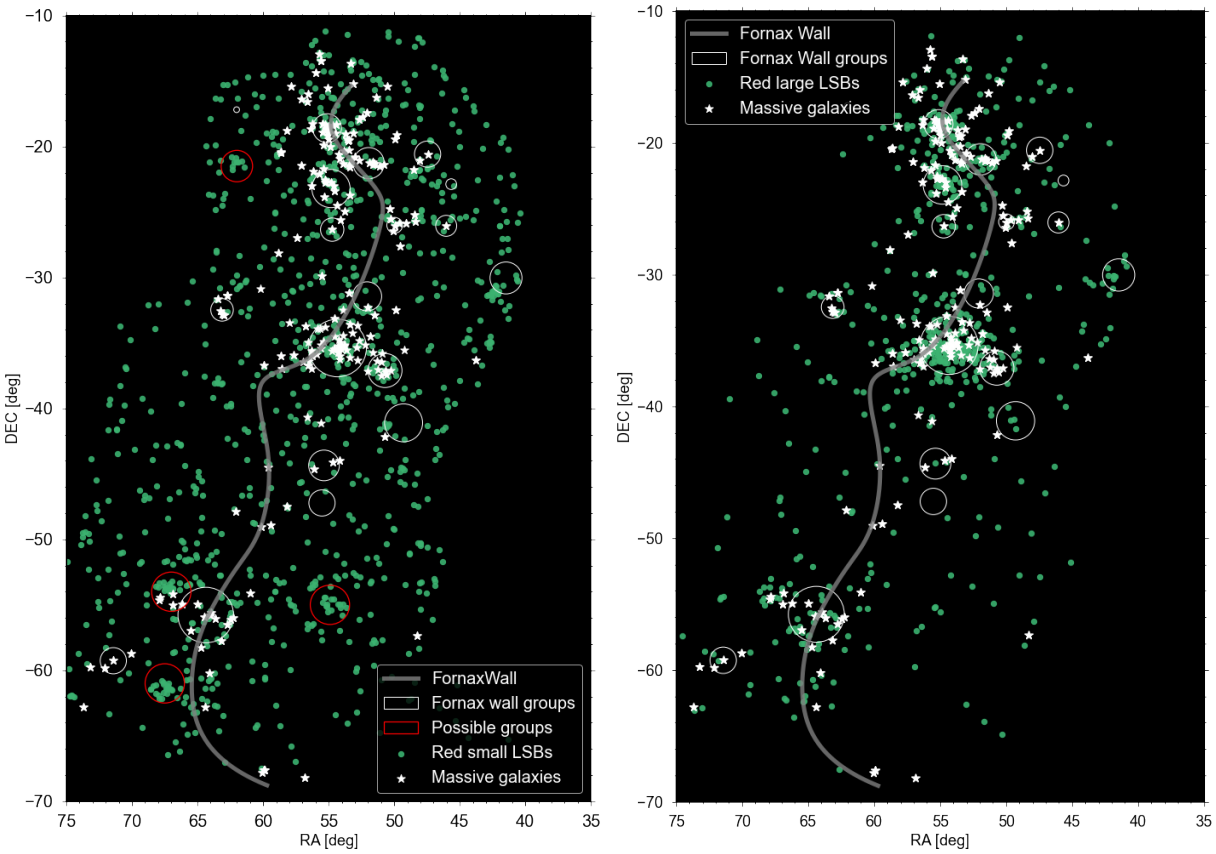

Figure 26: The 2D distribution of red LSBs with $R_{e,r} \leq 0.47$ kpc (left) and red LSBs with $R_{e,r} > 0.47$ kpc (right). Massive galaxies (R24) belonging to the Fornax Wall is included as white stars and Fornax Wall groups as white circles. The approximate location of some possible groups found in the distribution of red LSBs with $R_{e,r} > 0.47$ kpc is denoted by the red circles.

[6]Effective radius of LSBs have a range of $\sim 0.5 - 2$ kpc in Jackson et al. 2021

Our work supports their theory as nearly all large LSBs are found in or near groups that are close to the Fornax Wall. However, we do not have direct evidence that their progenitors formed in high density regions at high redshifts as they may have been accreted from nearby regions later (like the UDGs in Sales et al. 2020). It is likely that the large LSBs in the outskirts of groups are infalling galaxies. Therefore, it is still possible that they may have attained their size solely through tidal interactions with massive hosts and/or ram pressure stripping.

In summary, we find that nearly all red large LSBs are found within or near the Fornax Wall groups where there are BCGs and other massive galaxies, while small red LSBs dominate the pristine environment. In particular, the largest red LSBs are only found in groups. This likely supports the simulation by Jackson et al. 2021 which suggests that they were formed in high density environments through supernova feedback induced by the environment. Additional investigation is necessary to understand if large red LSBs are mainly influenced by the local environment (group and massive host galaxies) or if the large-scale assembly of galaxies and matter (infall or increased gas accretion at early epochs) is also important.

We also comment on the distribution of small red LSBs, as the presence of quenched LSBs in the pristine environment could present an interesting avenue for future research. In some regions, they seem to be clumped together (red circles Figure 26). These regions do not always have a massive galaxy in them (e.g., below the Dorado group, towards the left in the figure) and are not necessarily near known groups. We speculate that they may be dwarf-galaxy groups with no massive hosts like those observed by Tully et al. 2006. Further analysis is required to confirm if they form groups, if their star formation is quenched and to estimate if they may be precursors of pre-processed cluster galaxies.

5.2 Summary of Main Contributions

In this work, we explored the LSB dwarf galaxies in the Fornax-Eridanus supercluster using the spine of the Fornax Wall defined by R24. We obtained a supercluster low-surface brightness dwarf galaxy (SC dwarf) catalog by identifying Fornax Wall member galaxies from the DES LSB catalog using scaling relations, a known background/foreground group catalog and visual inspection. We calculated the absolute magnitude and stellar masses of the galaxies, and their distributions were in good agreement with literature. The SC dwarf catalog was estimated to contain mostly dEs and dIrrs based on the size-magnitude relation. We summarise the main results:

1. We investigated the clustering of red LSBs found in the DES survey by T21, in the context of the supercluster. Red LSBs ($g-r<0.45$ mag) dominated the group environment while blue LSBs dominated the pristine environment as determined by T21.

2. We find that the morphology of LSBs depends on their proximity to the Fornax Wall spine. Red LSBs were located close to the spine and their fraction decreased away from the spine.

3. The effective radius of red LSBs was found to depend on the environment. The largest red LSBs were in groups and were not found in the pristine environment.

The morphological segregation of massive galaxies in the Fornax Wall was attributed to pre-processing in groups and the inflow of galaxies from nearby structures by R24. Our work suggests that LSBs also follow a similar morphological segregation with more red LSBs found close to the spine indicating that pre-processing may play a role. In addition to this, we find that the environment in groups is

likely to increase the effective radius of red LSBs. As the largest LSBs are not found in the pristine environment, it is likely that the group environment plays a primary role in their formation.

5.3 Suggestions for future work

The SC dwarf catalog, while comprehensive, includes galaxies that are not LSBs, such as bright galaxies with Sérsic $n \sim 5$, and those with $\bar{\mu}_{e,r} > 23.5$ mag arcsec^{-2}. In addition to this, the T21 catalog, from which the SC dwarf catalog is derived, was dominated by blue galaxies. To enhance the accuracy of the galaxy properties and refine the purity of the LSB sample, it is crucial to redo their photometry. Furthermore, visual inspection of these galaxies will aid in verifying their morphology and color.

The DES Y3 GOLD catalog was found to have nearly 66% of the FDSDC catalog after applying only $\bar{\mu}_{e,r} > 24.2$ mag arcsec^{-2} and $R_{e,r} > 2.5$" (T21). The T21 catalog was made with strict selection effects and has $\sim$ 45% of the FDSDC catalog. Their catalog was produced after applying machine learning classification and additional cuts based on color. Nearly 20% of the galaxies found in DES Y3 GOLD are not in the T21 catalog. Using the DES Y3 GOLD catalog directly and identifying LSBs might improve its completeness.

The Euclid (Laureijs et al. 2011) mission surveys $\sim$ 15000 deg^2 area with high spatial resolution and depth that has not been achieved previously for wide surveys (Euclid Collaboration; Scaramella, R. et al. 2022). Imaging from Visual instrument (VIS; Cropper et al. 2014) in the optical band is able to resolve features in LSBs and may enable the use of surface brightness fluctuations to estimate distances to these galaxies (Cuillandre 2024). The advent of Euclid and future wide surveys with deep data will largely improve the identification of members of the Fornax Wall.

Analysing additional properties such as metallicity, asymmetry, and alignment of the galaxies can give deeper insights into their star formation histories and structure. Venhola et al. 2022 showed that dwarf galaxies with large excess size(the deviation of the effective radius of a galaxy from the mean at a given mass) had a weak preferential alignment towards the Fornax cluster center. Moreover, galaxies that have experienced tidal disturbances may be elongated towards the perturbation source. Investigating this can reveal whether the Fornax wall may have some (weak)influence on pristine LSBs and confirm whether pre-processing dictates the observed morphological distribution.

Applying a nearest-neighbor algorithm to detect possible groups of LSBs in the pristine environment can provide better insights on the mechanisms responsible for the properties of galaxies in them. Analysing filamentary structures detected by R24 around the Fornax Wall is also vital to understand the evolutionary pathway of galaxies and the subsequent environmental effects on LSBs, especially in the pristine environment.

Acknowledgments

I am deeply grateful for the guidance of my supervisors, Reynier and Angela, who have been persistently supportive and understanding throughout my journey. Their patience and encouragement have been crucial to my progress and completion of this thesis. I would like to thank our student advisor, Liisa, who encouraged me to persevere through difficult times. I am fortunate to have wonderful friends who were always ready to lend their ears when I needed them most. Throughout the journey of my thesis, I have experienced ups and downs which I could not have navigated without the aid of the people mentioned here. Thank you.

Appendix

A Comparison of rest-frame colors at different regions in the Fornax Wall

To justify the usage of the Fornax BCG to define background galaxies in the color-magnitude diagram for the supercluster galaxies, we calculate the rest-frame colors using K-correction, and compare the rest-frame colors of a particular apparent color when observed at the Fornax cluster and at the two extremities of the Fornax Wall. The galaxy magnitudes are K-corrected for a range of g-r and g-i colors using the empirical relations available in the python calculator provided by Chilingarian et al. 2010 and Chilingarian and Zolotukhin 2012. For the range of redshifts spanned by the Fornax Wall BCGs ($z \sim 0.004$ to $z \sim 0.006$; 2M++ catalog Lavaux and Hudson 2011), the rest-frame colors differ by 0.004 at maximum which is less than the errors[7] (order of 0.01) in LSB colors.

[7]Error in g - r color = $\sqrt{(e_g^2 + e_r^2)}$, where e_g and e_r are error in g and r magnitudes respectively.

Bibliography

N. C. Amorisco and A. Loeb. Ultradiffuse galaxies: the high-spin tail of the abundant dwarf galaxy population. *Monthly Notices of the Royal Astronomical Society*, 459(1):L51–L55, June 2016. doi: 10.1093/mnrasl/slw055.

Hong Bae Ann and Mira Seo. Morphology of Local Galaxies from SDSS. *Publication of Korean Astronomical Society*, 30(2):525–527, September 2015. doi: 10.5303/PKAS.2015.30.2.525.

Pablo A. Araya-Melo, Andreas Reisenegger, Andrés Meza, Rien van de Weygaert, Rolando Dünner, and Hernán Quintana. Future evolution of bound superclusters in an accelerating Universe. *Monthly Notices of the Royal Astronomical Society*, 399(1):97–120, October 2009. doi: 10.1111/j.1365-2966.2009.15292.x.

Yannick M. Bahé, Ian G. McCarthy, Michael L. Balogh, and Andreea S. Font. Why does the environmental influence on group and cluster galaxies extend beyond the virial radius? *Monthly Notices of the Royal Astronomical Society*, 430(4):3017–3031, April 2013. doi: 10.1093/mnras/stt109.

Andreas A. Berlind, Michael R. Blanton, David W. Hogg, David H. Weinberg, Romeel Davé, Daniel J. Eisenstein, and Neal Katz. Interpreting the Relationship between Galaxy Luminosity, Color, and Environment. *Astrophysical Journal*, 629(2):625–632, August 2005. doi: 10.1086/431658.

E. Bertin and S. Arnouts. SExtractor: Source Extractor. Astrophysics Source Code Library, record ascl:1010.064, October 2010.

Bahar Bidaran, Anna Pasquali, Thorsten Lisker, Lodovico Coccato, Jesus Falcón-Barroso, Glenn van de Ven, Reynier Peletier, Eric Emsellem, Eva K. Grebel, Francesco La Barbera, Joachim Janz, Agnieszka Sybilska, Rukmani Vijayaraghavan, III Gallagher, John, and Dimitri A. Gadotti. On the accretion of a new group of galaxies on to Virgo: I. Internal kinematics of nine in-falling dEs. *Monthly Notices of the Royal Astronomical Society*, 497(2):1904–1924, September 2020. doi: 10.1093/mnras/staa2097.

B. Binggeli, A. Sandage, and M. Tarenghi. Studies of the Virgo Cluster. I. Photometry of 109 galaxies near the cluster center to serve as standards. *Astronomical Journal*, 89:64–82, January 1984. doi: 10.1086/113484.

Bruno Binggeli, G. A. Tammann, and Allan Sandage. Studies of the Virgo Cluster. VI. Morphological and Kinematical Structure of the Virgo Cluster. *Astronomical Journal*, 94:251, August 1987. doi: 10.1086/114467.

Bruno Binggeli, Allan Sandage, and G. A. Tammann. The luminosity function of galaxies. *Annual Review of Astronomy and Astrophysics*, 26:509–560, January 1988. doi: 10.1146/annurev.aa.26.090188.002453.

Michael R. Blanton, David W. Hogg, Neta A. Bahcall, Ivan K. Baldry, J. Brinkmann, István Csabai, Daniel Eisenstein, Masataka Fukugita, James E. Gunn, Željko Ivezić, D. Q. Lamb, Robert H. Lupton, Jon Loveday, Jeffrey A. Munn, R. C. Nichol, Sadanori Okamura, David J. Schlegel, Kazuhiro Shimasaku, Michael A. Strauss, Michael S. Vogeley, and David H. Weinberg. The Broadband Optical Properties of Galaxies with Redshifts 0.02¡z¡0.22. *Astrophysical Journal*, 594(1):186–207, September 2003. doi: 10.1086/375528.

Michael R. Blanton, Robert H. Lupton, David J. Schlegel, Michael A. Strauss, J. Brinkmann, Masataka Fukugita, and Jon Loveday. The Properties and Luminosity Function of Extremely Low Luminosity Galaxies. *Astrophysical Journal*, 631(1):208–230, September 2005. doi: 10.1086/431416.

J. Richard Bond, Lev Kofman, and Dmitry Pogosyan. How filaments of galaxies are woven into the cosmic web. *Nature*, 380(6575):603–606, April 1996. doi: 10.1038/380603a0.

A. Boselli, S. Boissier, L. Cortese, and G. Gavazzi. The Origin of Dwarf Ellipticals in the Virgo Cluster. *Astrophysical Journal*, 674(2):742–767, February 2008. doi: 10.1086/525513.

G. D. Bothun, T. C. Beers, J. R. Mould, and J. P. Huchra. A redshift survey of low-surface-brightness galaxies. I. The basic data. *Astronomical Journal*, 90:2487–2494, December 1985. doi: 10.1086/113951.

Jean P. Brodie, Aaron J. Romanowsky, Jay Strader, and Duncan A. Forbes. The Relationships among Compact Stellar Systems: A Fresh View of Ultracompact Dwarfs. *Astronomical Journal*, 142(6):199, December 2011. doi: 10.1088/0004-6256/142/6/199.

Sarah Brough, Duncan A. Forbes, Virginia A. Kilborn, Warrick Couch, and Matthew Colless. Eridanus - a supergroup in the local Universe? *Monthly Notices of the Royal Astronomical Society*, 369(3):1351–1374, July 2006. doi: 10.1111/j.1365-2966.2006.10387.x.

Marius Cautun, Rien van de Weygaert, Bernard J. T. Jones, and Carlos S. Frenk. Evolution of the cosmic web. *Monthly Notices of the Royal Astronomical Society*, 441(4):2923–2973, July 2014. doi: 10.1093/mnras/stu768.

Renyue Cen, Ana Roxana Pop, and Neta A. Bahcall. Gas loss in simulated galaxies as they fall into clusters. *Proceedings of the National Academy of Science*, 111(22):7914–7919, June 2014. doi: 10.1073/pnas.1407300111.

Igor V. Chilingarian and Ivan Yu. Zolotukhin. A universal ultraviolet-optical colour-colour-magnitude relation of galaxies. *Monthly Notices of the Royal Astronomical Society*, 419(2):1727–1739, January 2012. doi: 10.1111/j.1365-2966.2011.19837.x.

Igor V. Chilingarian, Anne-Laure Melchior, and Ivan Yu. Zolotukhin. Analytical approximations of K-corrections in optical and near-infrared bands. *Monthly Notices of the Royal Astronomical Society*, 405(3):1409–1420, July 2010. doi: 10.1111/j.1365-2966.2010.16506.x.

Nelvy Choque-Challapa, J. Alfonso L. Aguerri, Pavel E. Mancera Piña, Reynier Peletier, Aku Venhola, and Marc Verheijen. The dwarf galaxy population in nearby clusters from the KIWICS survey. *Monthly Notices of the Royal Astronomical Society*, 507(4):6045–6060, November 2021. doi: 10.1093/mnras/stab2420.

Jiwon Chung, Suk Kim, Soo-Chang Rey, and Youngdae Lee. Star-forming Dwarf Galaxies in Filamentary Structures around the Virgo Cluster: Probing Chemical Pre-processing in Filament Environments. *Astrophysical Journal*, 923(2):235, December 2021. doi: 10.3847/1538-4357/ac3002.

Mark Cropper, S. Pottinger, S. M. Niemi, J. Denniston, R. Cole, M. Szafraniec, Y. Mellier, M. Berthé, J. Martignac, C. Cara, A. M. di Giorgio, A. Sciortino, S. Paltani, L. Genolet, J. J. Fourmand, M. Charra, P. Guttridge, B. Winter, J. Endicott, A. Holland, J. Gow, N. Murray, D. Hall, J. Amiaux, R. Laureijs, G. Racca, J. C. Salvignol, A. Short, J. Lorenzo Alvarez, T. Kitching, H. Hoekstra,

and R. Massey. VIS: the visible imager for Euclid. In Jr. Oschmann, Jacobus M., Mark Clampin, Giovanni G. Fazio, and Howard A. MacEwen, editors, *Space Telescopes and Instrumentation 2014: Optical, Infrared, and Millimeter Wave*, volume 9143 of *Society of Photo-Optical Instrumentation Engineers (SPIE) Conference Series*, page 91430J, August 2014. doi: 10.1117/12.2055543.

Jean-Charles Cuillandre. Euclid's view of the Low Surface Brightness universe: performance assessment through the Early Release Observations. In *EAS2024*, page 2660, July 2024.

V. de Lapparent, M. J. Geller, and J. P. Huchra. A Slice of the Universe. *Astrophysical Journal Letters*, 302:L1, March 1986. doi: 10.1086/184625.

I. De Looze, M. Baes, S. Zibetti, J. Fritz, L. Cortese, J. I. Davies, J. Verstappen, G. J. Bendo, S. Bianchi, M. Clemens, D. J. Bomans, A. Boselli, E. Corbelli, A. Dariush, S. di Serego Alighieri, D. Fadda, D. A. Garcia-Appadoo, G. Gavazzi, C. Giovanardi, M. Grossi, T. M. Hughes, L. K. Hunt, A. P. Jones, S. Madden, D. Pierini, M. Pohlen, S. Sabatini, M. W. L. Smith, C. Vlahakis, and E. M. Xilouris. The Herschel Virgo Cluster Survey . VII. Dust in cluster dwarf elliptical galaxies. *Astronomy and Astrophysics*, 518:L54, July 2010. doi: 10.1051/0004-6361/201014647.

S. de Rijcke, D. Michielsen, H. Dejonghe, W. W. Zeilinger, and G. K. T. Hau. Formation and evolution of dwarf elliptical galaxies. I. Structural and kinematical properties. *Astronomy and Astrophysics*, 438(2):491–505, August 2005. doi: 10.1051/0004-6361:20042213.

Gerard de Vaucouleurs. Evidence for a local super,galaxy. *Astronomical Journal*, 58:30, February 1953. doi: 10.1086/106805.

Gérard de Vaucouleurs. The distribution of bright galaxies and the local supergalaxy. *Vistas in Astronomy*, 2(1):1584–1606, January 1956. doi: 10.1016/0083-6656(56)90087-3.

Gerard de Vaucouleurs. The Local Supercluster of Galaxies. *Nature*, 182(4648):1478–1480, November 1958. doi: 10.1038/1821478a0.

Arianna Di Cintio, Chris B. Brook, Aaron A. Dutton, Andrea V. Macciò, Aura Obreja, and Avishai Dekel. NIHAO - XI. Formation of ultra-diffuse galaxies by outflows. *Monthly Notices of the Royal Astronomical Society*, 466(1):L1–L6, March 2017. doi: 10.1093/mnrasl/slw210.

Martina Donnari, Annalisa Pillepich, Gandhali D. Joshi, Dylan Nelson, Shy Genel, Federico Marinacci, Vicente Rodriguez-Gomez, Rüdiger Pakmor, Paul Torrey, Mark Vogelsberger, and Lars Hernquist. Quenched fractions in the IllustrisTNG simulations: the roles of AGN feedback, environment, and pre-processing. *Monthly Notices of the Royal Astronomical Society*, 500(3):4004–4024, January 2021. doi: 10.1093/mnras/staa3006.

A. Dressler. Galaxy morphology in rich clusters: implications for the formation and evolution of galaxies. *Astrophysical Journal*, 236:351–365, March 1980. doi: 10.1086/157753.

J. Einasto, M. Joeveer, and E. Saar. Structure of superclusters and supercluster formation. *Monthly Notices of the Royal Astronomical Society*, 193:353–375, November 1980. doi: 10.1093/mnras/193.2.353.

M. Einasto, E. Saar, J. Einasto, E. Tago, L. J. Liivam"agi, V. J. Martinez, J. L. Starck, V. M"uller, P. Hein"am"aki, P. Nurmi, M. Gramann, and G. H"utsi. The richest superclusters. II. Galaxy populations. *arXiv e-prints*, art. arXiv:0706.1126, June 2007. doi: 10.48550/arXiv.0706.1126.

M. Einasto, E. Saar, V. J. Martínez, J. Einasto, L. J. Liivamägi, E. Tago, J. L. Starck, V. Müller, P. Heinämäki, P. Nurmi, S. Paredes, M. Gramann, and G. Hütsi. Toward Understanding Rich Superclusters. *Astrophysical Journal*, 685(1):83–104, September 2008. doi: 10.1086/590374.

M. Einasto, E. Tago, E. Saar, P. Nurmi, I. Enkvist, P. Einasto, P. Heinämäki, L. J. Liivamägi, E. Tempel, J. Einasto, V. J. Martínez, J. Vennik, and P. Pihajoki. The Sloan great wall. Rich clusters. *Astronomy and Astrophysics*, 522:A92, November 2010. doi: 10.1051/0004-6361/201015165.

M. Einasto, L. J. Liivamägi, E. Tempel, E. Saar, J. Vennik, P. Nurmi, M. Gramann, J. Einasto, E. Tago, P. Heinämäki, A. Ahvensalmi, and V. J. Martínez. Multimodality of rich clusters from the SDSS DR8 within the supercluster-void network. *Astronomy and Astrophysics*, 542:A36, June 2012a. doi: 10.1051/0004-6361/201219119.

M. Einasto, L. J. Liivamägi, E. Tempel, E. Saar, J. Vennik, P. Nurmi, M. Gramann, J. Einasto, E. Tago, P. Heinämäki, A. Ahvensalmi, and V. J. Martínez. Multimodality of rich clusters from the SDSS DR8 within the supercluster-void network. *Astronomy and Astrophysics*, 542:A36, June 2012b. doi: 10.1051/0004-6361/201219119.

Maret Einasto and Jaan Einasto. Structure and formation of superclusters - VI. Morphology-density-luminosity relation of isolated and grouped galaxies. *Monthly Notices of the Royal Astronomical Society*, 226:543–562, June 1987. doi: 10.1093/mnras/226.3.543.

Maret Einasto, Heidi Lietzen, Mirt Gramann, Enn Saar, Elmo Tempel, Lauri Juhan Liivamägi, Antonio D. Montero-Dorta, Alina Streblyanska, Claudia Maraston, and José Alberto Rubiño-Martín. BOSS Great Wall: morphology, luminosity, and mass. *Astronomy and Astrophysics*, 603:A5, June 2017. doi: 10.1051/0004-6361/201629105.

Maret Einasto, Rain Kipper, Peeter Tenjes, Heidi Lietzen, Elmo Tempel, Lauri Juhan Liivamägi, Jaan Einasto, Antti Tamm, Pekka Heinämäki, and Pasi Nurmi. The Corona Borealis supercluster: connectivity, collapse, and evolution. *Astronomy and Astrophysics*, 649:A51, May 2021. doi: 10.1051/0004-6361/202040200.

Peter R. Eisenhardt, Roberto De Propris, Anthony H. Gonzalez, S. A. Stanford, Michael Wang, and Mark Dickinson. Multiaperture UBVRIzJHK Photometry of Galaxies in the Coma Cluster. *Astrophysical Journal Supplement*, 169(2):225–238, April 2007. doi: 10.1086/511688.

Euclid Collaboration; Scaramella, R., Amiaux, J., Mellier, Y., Burigana, C., Carvalho, C. S., Cuillandre, J.-C., Da Silva, A., Derosa, A., Dinis, J., Maiorano, E., Maris, M., Tereno, I., Laureijs, R., Boenke, T., Buenadicha, G., Dupac, X., Gaspar Venancio, L. M., Gómez-Álvarez, P., Hoar, J., Lorenzo Alvarez, J., Racca, G. D., Saavedra-Criado, G., Schwartz, J., Vavrek, R., Schirmer, M., Aussel, H., Azzollini, R., Cardone, V. F., Cropper, M., Ealet, A., Garilli, B., Gillard, W., Granett, B. R., Guzzo, L., Hoekstra, H., Jahnke, K., Kitching, T., Maciaszek, T., Meneghetti, M., Miller, L., Nakajima, R., Niemi, S. M., Pasian, F., Percival, W. J., Pottinger, S., Sauvage, M., Scodeggio, M., Wachter, S., Zacchei, A., Aghanim, N., Amara, A., Auphan, T., Auricchio, N., Awan, S., Balestra, A., Bender, R., Bodendorf, C., Bonino, D., Branchini, E., Brau-Nogue, S., Brescia, M., Candini, G. P., Capobianco, V., Carbone, C., Carlberg, R. G., Carretero, J., Casas, R., Castander, F. J., Castellano, M., Cavuoti, S., Cimatti, A., Cledassou, R., Congedo, G., Conselice, C. J., Conversi, L., Copin, Y., Corcione, L., Costille, A., Courbin, F., Degaudenzi, H., Douspis, M., Dubath, F., Duncan, C. A. J., Dusini, S., Farrens, S., Ferriol, S., Fosalba, P., Fourmanoit, N., Frailis, M., Franceschi, E., Franzetti, P., Fumana, M., Gillis, B., Giocoli, C., Grazian, A., Grupp,

F., Haugan, S. V. H., Holmes, W., Hormuth, F., Hudelot, P., Kermiche, S., Kiessling, A., Kilbinger, M., Kohley, R., Kubik, B., Kümmel, M., Kunz, M., Kurki-Suonio, H., Lahav, O., Ligori, S., Lilje, P. B., Lloro, I., Mansutti, O., Marggraf, O., Markovic, K., Marulli, F., Massey, R., Maurogordato, S., Melchior, M., Merlin, E., Meylan, G., Mohr, J. J., Moresco, M., Morin, B., Moscardini, L., Munari, E., Nichol, R. C., Padilla, C., Paltani, S., Peacock, J., Pedersen, K., Pettorino, V., Pires, S., Poncet, M., Popa, L., Pozzetti, L., Raison, F., Rebolo, R., Rhodes, J., Rix, H.-W., Roncarelli, M., Rossetti, E., Saglia, R., Schneider, P., Schrabback, T., Secroun, A., Seidel, G., Serrano, S., Sirignano, C., Sirri, G., Skottfelt, J., Stanco, L., Starck, J. L., Tallada-Crespí, P., Tavagnacco, D., Taylor, A. N., Teplitz, H. I., Toledo-Moreo, R., Torradeflot, F., Trifoglio, M., Valentijn, E. A., Valenziano, L., Verdoes Kleijn, G. A., Wang, Y., Welikala, N., Weller, J., Wetzstein, M., Zamorani, G., Zoubian, J., Andreon, S., Baldi, M., Bardelli, S., Boucaud, A., Camera, S., Di Ferdinando, D., Fabbian, G., Farinelli, R., Galeotta, S., Graciá-Carpio, J., Maino, D., Medinaceli, E., Mei, S., Neissner, C., Polenta, G., Renzi, A., Romelli, E., Rosset, C., Sureau, F., Tenti, M., Vassallo, T., Zucca, E., Baccigalupi, C., Balaguera-Antolínez, A., Battaglia, P., Biviano, A., Borgani, S., Bozzo, E., Cabanac, R., Cappi, A., Casas, S., Castignani, G., Colodro-Conde, C., Coupon, J., Courtois, H. M., Cuby, J., de la Torre, S., Desai, S., Dole, H., Fabricius, M., Farina, M., Ferreira, P. G., Finelli, F., Flose-Reimberg, P., Fotopoulou, S., Ganga, K., Gozaliasl, G., Hook, I. M., Keihanen, E., Kirkpatrick, C. C., Liebing, P., Lindholm, V., Mainetti, G., Martinelli, M., Martinet, N., Maturi, M., McCracken, H. J., Metcalf, R. B., Morgante, G., Nightingale, J., Nucita, A., Patrizii, L., Potter, D., Riccio, G., Sánchez, A. G., Sapone, D., Schewtschenko, J. A., Schultheis, M., Scottez, V., Teyssier, R., Tutusaus, I., Valiviita, J., Viel, M., Vriend, W., and Whittaker, L. Euclid preparation - i. the euclid wide survey. *AA*, 662:A112, 2022. doi: 10.1051/0004-6361/202141938. URL `https://doi.org/10.1051/0004-6361/202141938`.

A. P. Fairall, W. R. Paverd, and R. P. Ashley. Visualization of Nearby Large-Scale Structures. In Chantal Balkowski and R. C. Kraan-Korteweg, editors, *Unveiling Large-Scale Structures Behind the Milky Way*, volume 67 of *Astronomical Society of the Pacific Conference Series*, page 21, January 1994.

B. Flaugher, H. T. Diehl, K. Honscheid, T. M. C. Abbott, O. Alvarez, R. Angstadt, J. T. Annis, M. Antonik, O. Ballester, L. Beaufore, G. M. Bernstein, R. A. Bernstein, B. Bigelow, M. Bonati, D. Boprie, D. Brooks, E. J. Buckley-Geer, J. Campa, L. Cardiel-Sas, F. J. Castander, J. Castilla, H. Cease, J. M. Cela-Ruiz, S. Chappa, E. Chi, C. Cooper, L. N. da Costa, E. Dede, G. Derylo, D. L. DePoy, J. de Vicente, P. Doel, A. Drlica-Wagner, J. Eiting, A. E. Elliott, J. Emes, J. Estrada, A. Fausti Neto, D. A. Finley, R. Flores, J. Frieman, D. Gerdes, M. D. Gladders, B. Gregory, G. R. Gutierrez, J. Hao, S. E. Holland, S. Holm, D. Huffman, C. Jackson, D. J. James, M. Jonas, A. Karcher, I. Karliner, S. Kent, R. Kessler, M. Kozlovsky, R. G. Kron, D. Kubik, K. Kuehn, S. Kuhlmann, K. Kuk, O. Lahav, A. Lathrop, J. Lee, M. E. Levi, P. Lewis, T. S. Li, I. Mandrichenko, J. L. Marshall, G. Martinez, K. W. Merritt, R. Miquel, F. Muñoz, E. H. Neilsen, R. C. Nichol, B. Nord, R. Ogando, J. Olsen, N. Palaio, K. Patton, J. Peoples, A. A. Plazas, J. Rauch, K. Reil, J. P. Rheault, N. A. Roe, H. Rogers, A. Roodman, E. Sanchez, V. Scarpine, R. H. Schindler, R. Schmidt, R. Schmitt, M. Schubnell, K. Schultz, P. Schurter, L. Scott, S. Serrano, T. M. Shaw, R. C. Smith, M. Soares-Santos, A. Stefanik, W. Stuermer, E. Suchyta, A. Sypniewski, G. Tarle, J. Thaler, R. Tighe, C. Tran, D. Tucker, A. R. Walker, G. Wang, M. Watson, C. Weaverdyck, W. Wester, R. Woods, B. Yanny, and DES Collaboration. The Dark Energy Camera. *Astronomical Journal*, 150(5):150, November 2015. doi: 10.1088/0004-6256/150/5/150.

B. Q. For, K. Spekkens, L. Staveley-Smith, K. Bekki, A. Karunakaran, B. Catinella, B. S. Koribalski,

K. Lee-Waddell, J. P. Madrid, C. Murugeshan, J. Rhee, T. Westmeier, O. I. Wong, D. Zaritsky, and R. Donnerstein. WALLABY pre-pilot survey: ultra-diffuse galaxies in the Eridanus supergroup. *Monthly Notices of the Royal Astronomical Society*, 526(2):3130–3140, December 2023. doi: 10.1093/mnras/stad2921.

Christopher T. Garling, Annika H. G. Peter, Christopher S. Kochanek, David J. Sand, and Denija Crnojević. The case for strangulation in low-mass hosts: DDO 113. *Monthly Notices of the Royal Astronomical Society*, 492(2):1713–1730, February 2020. doi: 10.1093/mnras/stz3526.

M. Geha, M. R. Blanton, R. Yan, and J. L. Tinker. A Stellar Mass Threshold for Quenching of Field Galaxies. *Astrophysical Journal*, 757(1):85, September 2012. doi: 10.1088/0004-637X/757/1/85.

Margaret J. Geller, Antonaldo Diaferio, Michael J. Kurtz, Ian P. Dell'Antonio, and Daniel G. Fabricant. The Faint End of the Luminosity Function and Low Surface Brightness Galaxies. *Astronomical Journal*, 143(4):102, April 2012. doi: 10.1088/0004-6256/143/4/102.

Johnny P. Greco, Jenny E. Greene, Michael A. Strauss, Lauren A. Macarthur, Xzavier Flowers, Andy D. Goulding, Song Huang, Ji Hoon Kim, Yutaka Komiyama, Alexie Leauthaud, Lukas Leisman, Robert H. Lupton, Cristóbal Sifón, and Shiang-Yu Wang. Illuminating Low Surface Brightness Galaxies with the Hyper Suprime-Cam Survey. *Astrophysical Journal*, 857(2):104, April 2018. doi: 10.3847/1538-4357/aab842.

C. P. Haines, M. J. Pereira, G. P. Smith, E. Egami, A. Babul, A. Finoguenov, F. Ziparo, S. L. McGee, T. D. Rawle, N. Okabe, and S. M. Moran. LoCuSS: The Slow Quenching of Star Formation in Cluster Galaxies and the Need for Pre-processing. *Astrophysical Journal*, 806(1):101, June 2015. doi: 10.1088/0004-637X/806/1/101.

C. P. Haines, G. Busarello, P. Merluzzi, K. A. Pimbblet, F. P. A. Vogt, M. A. Dopita, A. Mercurio, A. Grado, and L. Limatola. Shapley Supercluster Survey: mapping the filamentary network connecting the clusters. *Monthly Notices of the Royal Astronomical Society*, 481(1):1055–1074, November 2018. doi: 10.1093/mnras/sty2338.

E. Hamraz, R. F. Peletier, H. G. Khosroshahi, E. A. Valentijn, M. den Brok, and A. Venhola. Young stellar populations in early-type dwarf galaxies. Occurrence, radial extent, and scaling relations. *Astronomy and Astrophysics*, 625:A94, May 2019. doi: 10.1051/0004-6361/201935076.

J. L. Hinz, M. J. Rieke, G. H. Rieke, C. N. A. Willmer, K. Misselt, C. W. Engelbracht, M. Blaylock, and T. E. Pickering. Spitzer Observations of Low-Luminosity Isolated and Low Surface Brightness Galaxies. *Astrophysical Journal*, 663(2):895–907, July 2007. doi: 10.1086/518817.

J. Huchra, M. Davis, D. Latham, and J. Tonry. A survey of galaxy redshifts. IV - The data. *Astrophysical Journal Supplement*, 52:89–119, June 1983. doi: 10.1086/190860.

E. Iodice, M. Cantiello, M. Hilker, M. Rejkuba, M. Arnaboldi, M. Spavone, L. Greggio, D. A. Forbes, G. D'Ago, S. Mieske, C. Spiniello, A. La Marca, R. Rampazzo, M. Paolillo, M. Capaccioli, and P. Schipani. The first detection of ultra-diffuse galaxies in the Hydra I cluster from the VEGAS survey. *Astronomy and Astrophysics*, 642:A48, October 2020. doi: 10.1051/0004-6361/202038523.

R. A. Jackson, G. Martin, S. Kaviraj, M. Ramsøy, J. E. G. Devriendt, T. Sedgwick, C. Laigle, H. Choi, R. S. Beckmann, M. Volonteri, Y. Dubois, C. Pichon, S. K. Yi, A. Slyz, K. Kraljic, T. Kimm, S. Peirani, and I. Baldry. The origin of low-surface-brightness galaxies in the dwarf

regime. *Monthly Notices of the Royal Astronomical Society*, 502(3):4262–4276, April 2021. doi: 10.1093/mnras/stab077.

Sebastian Jester, Donald P. Schneider, Gordon T. Richards, Richard F. Green, Maarten Schmidt, Patrick B. Hall, Michael A. Strauss, Daniel E. Vanden Berk, Chris Stoughton, James E. Gunn, Jon Brinkmann, Stephen M. Kent, J. Allyn Smith, Douglas L. Tucker, and Brian Yanny. The Sloan Digital Sky Survey View of the Palomar-Green Bright Quasar Survey. *Astronomical Journal*, 130 (3):873–895, September 2005. doi: 10.1086/432466.

Michael G. Jones, Paul Bennet, Burçin Mutlu-Pakdil, David J. Sand, Kristine Spekkens, Denija Crnojević, Ananthan Karunakaran, and Dennis Zaritsky. Evidence for Ultra-diffuse Galaxy Formation through Tidal Heating of Normal Dwarfs. *Astrophysical Journal*, 919(2):72, October 2021. doi: 10.3847/1538-4357/ac0975.

Junais, K. Małek, S. Boissier, W. J. Pearson, A. Pollo, A. Boselli, M. Boquien, D. Donevski, T. Goto, M. Hamed, S. J. Kim, J. Koda, H. Matsuhara, G. Riccio, and M. Romano. Variation in optical and infrared properties of galaxies in relation to their surface brightness. *Astronomy and Astrophysics*, 676:A41, August 2023. doi: 10.1051/0004-6361/202346528.

Mina Koleva, Philippe Prugniel, Sven De Rijcke, and Werner W. Zeilinger. Age and metallicity gradients in early-type galaxies: a dwarf-to-giant sequence. *Monthly Notices of the Royal Astronomical Society*, 417(3):1643–1671, November 2011. doi: 10.1111/j.1365-2966.2011.19057.x.

J. Kormendy. Families of ellipsoidal stellar systems and the formation of dwarf elliptical galaxies. *Astrophysical Journal*, 295:73–79, August 1985. doi: 10.1086/163350.

John Kormendy and Ralf Bender. A Revised Parallel-sequence Morphological Classification of Galaxies: Structure and Formation of S0 and Spheroidal Galaxies. *Astrophysical Journal Supplement*, 198(1):2, January 2012. doi: 10.1088/0067-0049/198/1/2.

Ehsan Kourkchi and R. Brent Tully. Galaxy Groups Within 3500 km s^{-1}. *Astrophysical Journal*, 843 (1):16, July 2017. doi: 10.3847/1538-4357/aa76db.

R. Laureijs, J. Amiaux, S. Arduini, J. L. Augueres, J. Brinchmann, R. Cole, M. Cropper, C. Dabin, L. Duvet, A. Ealet, B. Garilli, P. Gondoin, L. Guzzo, J. Hoar, H. Hoekstra, R. Holmes, T. Kitching, T. Maciaszek, Y. Mellier, F. Pasian, W. Percival, J. Rhodes, G. Saavedra Criado, M. Sauvage, R. Scaramella, L. Valenziano, S. Warren, R. Bender, F. Castander, A. Cimatti, O. Le Fèvre, H. Kurki-Suonio, M. Levi, P. Lilje, G. Meylan, R. Nichol, K. Pedersen, V. Popa, R. Rebolo Lopez, H. W. Rix, H. Rottgering, W. Zeilinger, F. Grupp, P. Hudelot, R. Massey, M. Meneghetti, L. Miller, S. Paltani, S. Paulin-Henriksson, S. Pires, C. Saxton, T. Schrabback, G. Seidel, J. Walsh, N. Aghanim, L. Amendola, J. Bartlett, C. Baccigalupi, J. P. Beaulieu, K. Benabed, J. G. Cuby, D. Elbaz, P. Fosalba, G. Gavazzi, A. Helmi, I. Hook, M. Irwin, J. P. Kneib, M. Kunz, F. Mannucci, L. Moscardini, C. Tao, R. Teyssier, J. Weller, G. Zamorani, M. R. Zapatero Osorio, O. Boulade, J. J. Foumond, A. Di Giorgio, P. Guttridge, A. James, M. Kemp, J. Martignac, A. Spencer, D. Walton, T. Blümchen, C. Bonoli, F. Bortoletto, C. Cerna, L. Corcione, C. Fabron, K. Jahnke, S. Ligori, F. Madrid, L. Martin, G. Morgante, T. Pamplona, E. Prieto, M. Riva, R. Toledo, M. Trifoglio, F. Zerbi, F. Abdalla, M. Douspis, C. Grenet, S. Borgani, R. Bouwens, F. Courbin, J. M. Delouis, P. Dubath, A. Fontana, M. Frailis, A. Grazian, J. Koppenhöfer, O. Mansutti, M. Melchior, M. Mignoli, J. Mohr, C. Neissner, K. Noddle, M. Poncet, M. Scodeggio, S. Serrano, N. Shane, J. L. Starck, C. Surace, A. Taylor, G. Verdoes-Kleijn, C. Vuerli, O. R. Williams, A. Zacchei, B. Altieri,

I. Escudero Sanz, R. Kohley, T. Oosterbroek, P. Astier, D. Bacon, S. Bardelli, C. Baugh, F. Bellagamba, C. Benoist, D. Bianchi, A. Biviano, E. Branchini, C. Carbone, V. Cardone, D. Clements, S. Colombi, C. Conselice, G. Cresci, N. Deacon, J. Dunlop, C. Fedeli, F. Fontanot, P. Franzetti, C. Giocoli, J. Garcia-Bellido, J. Gow, A. Heavens, P. Hewett, C. Heymans, A. Holland, Z. Huang, O. Ilbert, B. Joachimi, E. Jennins, E. Kerins, A. Kiessling, D. Kirk, R. Kotak, O. Krause, O. Lahav, F. van Leeuwen, J. Lesgourgues, M. Lombardi, M. Magliocchetti, K. Maguire, E. Majerotto, R. Maoli, F. Marulli, S. Maurogordato, H. McCracken, R. McLure, A. Melchiorri, A. Merson, M. Moresco, M. Nonino, P. Norberg, J. Peacock, R. Pello, M. Penny, V. Pettorino, C. Di Porto, L. Pozzetti, C. Quercellini, M. Radovich, A. Rassat, N. Roche, S. Ronayette, E. Rossetti, B. Sartoris, P. Schneider, E. Semboloni, S. Serjeant, F. Simpson, C. Skordis, G. Smadja, S. Smartt, P. Spano, S. Spiro, M. Sullivan, A. Tilquin, R. Trotta, L. Verde, Y. Wang, G. Williger, G. Zhao, J. Zoubian, and E. Zucca. Euclid Definition Study Report. *arXiv e-prints*, art. arXiv:1110.3193, October 2011. doi: 10.48550/arXiv.1110.3193.

Guilhem Lavaux and Michael J. Hudson. The 2M++ galaxy redshift catalogue. *Monthly Notices of the Royal Astronomical Society*, 416(4):2840–2856, October 2011. doi: 10.1111/j.1365-2966.2011.19233.x.

Youngdae Lee, Suk Kim, Soo-Chang Rey, and Jiwon Chung. Properties of Galaxies in Cosmic Filaments around the Virgo Cluster. *Astrophysical Journal*, 906(2):68, January 2021. doi: 10.3847/1538-4357/abcaa0.

Luke Leisman, Martha P. Haynes, Riccardo Giovanelli, and ALFALFA Almost Darks Team. (Almost) Dark Galaxies in the ALFALFA Survey: HI-bearing Ultra-Diffuse Galaxies, and Beyond. In *American Astronomical Society Meeting Abstracts #229*, volume 229 of *American Astronomical Society Meeting Abstracts*, page 132.06, January 2017.

Y. C. Liang, G. H. Zhong, F. Hammer, X. Y. Chen, F. S. Liu, D. Gao, J. Y. Hu, L. C. Deng, and B. Zhang. A large sample of low surface brightness disc galaxies from the SDSS - II. Metallicities in surface brightness bins. *Monthly Notices of the Royal Astronomical Society*, 409(1):213–225, November 2010. doi: 10.1111/j.1365-2966.2010.16891.x.

Thorsten Lisker, Katharina Glatt, Pieter Westera, and Eva K. Grebel. Virgo Cluster Early-Type Dwarf Galaxies with the Sloan Digital Sky Survey. II. Early-Type Dwarfs with Central Star Formation. *Astronomical Journal*, 132(6):2432–2452, December 2006. doi: 10.1086/508414.

Thorsten Lisker, Rukmani Vijayaraghavan, Joachim Janz, III Gallagher, John S., Christoph Engler, and Linda Urich. The Active Assembly of the Virgo Cluster: Indications for Recent Group Infall From Early-type Dwarf Galaxies. *Astrophysical Journal*, 865(1):40, September 2018. doi: 10.3847/1538-4357/aadae1.

Smriti Mahajan, Chris P. Haines, and Somak Raychaudhury. Star formation, starbursts and quenching across the Coma supercluster. *Monthly Notices of the Royal Astronomical Society*, 404(4):1745–1760, June 2010. doi: 10.1111/j.1365-2966.2010.16432.x.

Smriti Mahajan, Chris P. Haines, and Somak Raychaudhury. The evolution of dwarf galaxies in the Coma supercluster. *Monthly Notices of the Royal Astronomical Society*, 412(2):1098–1104, April 2011. doi: 10.1111/j.1365-2966.2010.17977.x.

Smriti Mahajan, Somak Raychaudhury, and Kevin A. Pimbblet. Plunging fireworks: why do infalling galaxies light up on the outskirts of clusters? *Monthly Notices of the Royal Astronomical Society*, 427(2):1252–1265, December 2012. doi: 10.1111/j.1365-2966.2012.22059.x.

Dmitry Makarov and Igor Karachentsev. Galaxy groups and clouds in the local (z$\sim$ 0.01) Universe. *Monthly Notices of the Royal Astronomical Society*, 412(4):2498–2520, April 2011. doi: 10.1111/j.1365-2966.2010.18071.x.

G. Martin, S. Kaviraj, C. Laigle, J. E. G. Devriendt, R. A. Jackson, S. Peirani, Y. Dubois, C. Pichon, and A. Slyz. The formation and evolution of low-surface-brightness galaxies. *Monthly Notices of the Royal Astronomical Society*, 485(1):796–818, May 2019. doi: 10.1093/mnras/stz356.

Hagen T. Meyer, Thorsten Lisker, Joachim Janz, and Polychronis Papaderos. What will blue compact dwarf galaxies evolve into? *Astronomy and Astrophysics*, 562:A49, February 2014. doi: 10.1051/0004-6361/201220700.

Millennium Simulation Project. Millennium simulation project posters. `http://www.millennium-simulation.org/posters.html`. Accessed: 2024-08-04.

Shyamal Mitra. The Southern Supercluster. *Astronomical Journal*, 98:1175, October 1989. doi: 10.1086/115205.

Jae Yeon Mun, Ho Seong Hwang, Myung Gyoon Lee, Aeree Chung, Hyein Yoon, and Jong Chul Lee. Star Formation Activity of Galaxies Undergoing Ram Pressure Stripping in the Virgo Cluster. *Journal of Korean Astronomical Society*, 54:17–35, February 2021. doi: 10.5303%2FJKAS.2021.54.1.17.

O. G. Nasonova, J. A. de Freitas Pacheco, and I. D. Karachentsev. Hubble flow around Fornax cluster of galaxies. *Astronomy and Astrophysics*, 532:A104, August 2011. doi: 10.1051/0004-6361/201016004.

S. Paul, R. S. John, P. Gupta, and H. Kumar. Understanding 'galaxy groups' as a unique structure in the universe. *Monthly Notices of the Royal Astronomical Society*, 471(1):2–11, October 2017. doi: 10.1093/mnras/stx1488.

P. J. E. Peebles. Statistics of the distribution of galaxies. In J. Ehlers, J. J. Perry, and M. Walker, editors, *Ninth Texas Symposium on Relativistic Astrophysics*, volume 336, pages 161–171, February 1980. doi: 10.1111/j.1749-6632.1980.tb15927.x.

Ying-jie Peng, Simon J. Lilly, Katarina Kovač, Micol Bolzonella, Lucia Pozzetti, Alvio Renzini, Gianni Zamorani, Olivier Ilbert, Christian Knobel, Angela Iovino, Christian Maier, Olga Cucciati, Lidia Tasca, C. Marcella Carollo, John Silverman, Pawel Kampczyk, Loic de Ravel, David Sanders, Nicholas Scoville, Thierry Contini, Vincenzo Mainieri, Marco Scodeggio, Jean-Paul Kneib, Olivier Le Fèvre, Sandro Bardelli, Angela Bongiorno, Karina Caputi, Graziano Coppa, Sylvain de la Torre, Paolo Franzetti, Bianca Garilli, Fabrice Lamareille, Jean-Francois Le Borgne, Vincent Le Brun, Marco Mignoli, Enrique Perez Montero, Roser Pello, Elena Ricciardelli, Masayuki Tanaka, Laurence Tresse, Daniela Vergani, Niraj Welikala, Elena Zucca, Pascal Oesch, Ummi Abbas, Luke Barnes, Rongmon Bordoloi, Dario Bottini, Alberto Cappi, Paolo Cassata, Andrea Cimatti, Marco Fumana, Gunther Hasinger, Anton Koekemoer, Alexei Leauthaud, Dario Maccagni, Christian Marinoni, Henry McCracken, Pierdomenico Memeo, Baptiste Meneux, Preethi Nair, Cristiano

Porciani, Valentina Presotto, and Roberto Scaramella. Mass and Environment as Drivers of Galaxy Evolution in SDSS and zCOSMOS and the Origin of the Schechter Function. *Astrophysical Journal*, 721(1):193–221, September 2010. doi: 10.1088/0004-637X/721/1/193.

J. Price, S. Phillipps, A. Huxor, N. Trentham, H. C. Ferguson, R. O. Marzke, A. Hornschemeier, P. Goudfrooij, D. Hammer, R. B. Tully, K. Chiboucas, R. J. Smith, D. Carter, D. Merritt, M. Balcells, P. Erwin, and T. H. Puzia. The HST/ACS Coma Cluster Survey - V. Compact stellar systems in the Coma Cluster. *Monthly Notices of the Royal Astronomical Society*, 397(4):1816–1835, August 2009. doi: 10.1111/j.1365-2966.2009.15122.x.

Maria Angela Raj, Petra Awad, Reynier F. Peletier, Rory Smith, Ulrike Kuchner, Rien van de Weygaert, Noam I. Libeskind, Marco Canducci, Peter Tino, and Kerstin Bunte. The large-scale structure around the fornax-eridanus complex, 2024. URL `https://arxiv.org/abs/2407.03225`.

Javier Román and Ignacio Trujillo. Ultra-diffuse galaxies outside clusters: clues to their formation and evolution. *Monthly Notices of the Royal Astronomical Society*, 468(4):4039–4047, July 2017. doi: 10.1093/mnras/stx694.

Javier Román, Michael A. Beasley, Tomás Ruiz-Lara, and David Valls-Gabaud. Discovery of a red ultra-diffuse galaxy in a nearby void based on its globular cluster luminosity function. *Monthly Notices of the Royal Astronomical Society*, 486(1):823–835, June 2019. doi: 10.1093/mnras/stz835.

Javier Román, Michael G. Jones, Mireia Montes, Lourdes Verdes-Montenegro, Julián Garrido, and Susana Sánchez. A diffuse tidal dwarf galaxy destined to fade out as a "dark galaxy". *Astronomy and Astrophysics*, 649:L14, May 2021. doi: 10.1051/0004-6361/202141001.

Laura V. Sales, Julio F. Navarro, Louis Peñafiel, Eric W. Peng, Sungsoon Lim, and Lars Hernquist. The formation of ultradiffuse galaxies in clusters. *Monthly Notices of the Royal Astronomical Society*, 494(2):1848–1858, May 2020. doi: 10.1093/mnras/staa854.

A. Sandage and B. Binggeli. Studies of the Virgo cluster. III. A classification system and an illustrated Atlas of Virgo cluster dwarf galaxies. *Astronomical Journal*, 89:919–931, July 1984. doi: 10.1086/113588.

Mira Seo and Hong Bae Ann. Star formation histories of dwarf spheroidal and dwarf elliptical galaxies in the local Universe. *Monthly Notices of the Royal Astronomical Society*, 520(4):5521–5535, April 2023. doi: 10.1093/mnras/stad425.

Ramin A. Skibba, Steven P. Bamford, Robert C. Nichol, Chris J. Lintott, Dan Andreescu, Edward M. Edmondson, Phil Murray, M. Jordan Raddick, Kevin Schawinski, Anže Slosar, Alexander S. Szalay, Daniel Thomas, and Jan Vandenberg. Galaxy Zoo: disentangling the environmental dependence of morphology and colour. *Monthly Notices of the Royal Astronomical Society*, 399(2):966–982, October 2009. doi: 10.1111/j.1365-2966.2009.15334.x.

R. Smith, R. Sánchez-Janssen, M. A. Beasley, G. N. Candlish, B. K. Gibson, T. H. Puzia, J. Janz, A. Knebe, J. A. L. Aguerri, T. Lisker, G. Hensler, M. Fellhauer, L. Ferrarese, and S. K. Yi. The sensitivity of harassment to orbit: mass loss from early-type dwarfs in galaxy clusters. *Monthly Notices of the Royal Astronomical Society*, 454(3):2502–2516, December 2015. doi: 10.1093/mnras/stv2082.

Volker Springel, Simon D. M. White, Adrian Jenkins, Carlos S. Frenk, Naoki Yoshida, Liang Gao, Julio Navarro, Robert Thacker, Darren Croton, John Helly, John A. Peacock, Shaun Cole, Peter Thomas, Hugh Couchman, August Evrard, Jörg Colberg, and Frazer Pearce. Simulations of the formation, evolution and clustering of galaxies and quasars. *Nature*, 435(7042):629–636, June 2005a. doi: 10.1038/nature03597.

Volker Springel, Simon D. M. White, Adrian Jenkins, Carlos S. Frenk, Naoki Yoshida, Liang Gao, Julio Navarro, Robert Thacker, Darren Croton, John Helly, John A. Peacock, Shaun Cole, Peter Thomas, Hugh Couchman, August Evrard, Jörg Colberg, and Frazer Pearce. Simulations of the formation, evolution and clustering of galaxies and quasars. *Nature*, 435(7042):629–636, June 2005b. doi: 10.1038/nature03597.

A. H. Su, H. Salo, J. Janz, E. Laurikainen, A. Venhola, R. F. Peletier, E. Iodice, M. Hilker, M. Cantiello, N. Napolitano, M. Spavone, M. A. Raj, G. van de Ven, S. Mieske, M. Paolillo, M. Capaccioli, E. A. Valentijn, and A. E. Watkins. The Fornax Deep Survey (FDS) with the VST. XI. The search for signs of preprocessing between the Fornax main cluster and Fornax A group. *Astronomy and Astrophysics*, 647:A100, March 2021. doi: 10.1051/0004-6361/202039633.

Alan H. Su, Heikki Salo, Joachim Janz, Aku Venhola, and Reynier F. Peletier. Photometric properties of nuclear star clusters and their host galaxies in the Fornax cluster. *Astronomy and Astrophysics*, 664:A167, August 2022. doi: 10.1051/0004-6361/202142593.

D. Tanoglidis, A. Drlica-Wagner, K. Wei, T. S. Li, J. Sánchez, Y. Zhang, A. H. G. Peter, A. Feldmeier-Krause, J. Prat, K. Casey, A. Palmese, C. Sánchez, J. DeRose, C. Conselice, L. Gagnon, T. M. C. Abbott, M. Aguena, S. Allam, S. Avila, K. Bechtol, E. Bertin, S. Bhargava, D. Brooks, D. L. Burke, A. Carnero Rosell, M. Carrasco Kind, J. Carretero, C. Chang, M. Costanzi, L. N. da Costa, J. De Vicente, S. Desai, H. T. Diehl, P. Doel, T. F. Eifler, S. Everett, A. E. Evrard, B. Flaugher, J. Frieman, J. García-Bellido, D. W. Gerdes, R. A. Gruendl, J. Gschwend, G. Gutierrez, W. G. Hartley, D. L. Hollowood, D. Huterer, D. J. James, E. Krause, K. Kuehn, N. Kuropatkin, M. A. G. Maia, M. March, J. L. Marshall, F. Menanteau, R. Miquel, R. L. C. Ogando, F. Paz-Chinchón, A. K. Romer, A. Roodman, E. Sanchez, V. Scarpine, S. Serrano, I. Sevilla-Noarbe, M. Smith, E. Suchyta, G. Tarle, D. Thomas, D. L. Tucker, A. R. Walker, and DES Collaboration. Shadows in the Dark: Low-surface-brightness Galaxies Discovered in the Dark Energy Survey. *Astrophysical Journal Supplement*, 252(2):18, February 2021. doi: 10.3847/1538-4365/abca89.

Edward N. Taylor, Andrew M. Hopkins, Ivan K. Baldry, Michael J. I. Brown, Simon P. Driver, Lee S. Kelvin, David T. Hill, Aaron S. G. Robotham, Joss Bland-Hawthorn, D. H. Jones, R. G. Sharp, Daniel Thomas, Jochen Liske, Jon Loveday, Peder Norberg, J. A. Peacock, Steven P. Bamford, Sarah Brough, Matthew Colless, Ewan Cameron, Christopher J. Conselice, Scott M. Croom, C. S. Frenk, Madusha Gunawardhana, Konrad Kuijken, R. C. Nichol, H. R. Parkinson, S. Phillipps, K. A. Pimbblet, C. C. Popescu, Matthew Prescott, W. J. Sutherland, R. J. Tuffs, Eelco van Kampen, and D. Wijesinghe. Galaxy And Mass Assembly (GAMA): stellar mass estimates. *Monthly Notices of the Royal Astronomical Society*, 418(3):1587–1620, December 2011. doi: 10.1111/j.1365-2966.2011.19536.x.

M. B. Taylor. TOPCAT & STIL: Starlink Table/VOTable Processing Software. In P. Shopbell, M. Britton, and R. Ebert, editors, *Astronomical Data Analysis Software and Systems XIV*, volume 347 of *Astronomical Society of the Pacific Conference Series*, page 29, December 2005.

E. Tempel, J. Einasto, M. Einasto, E. Saar, and E. Tago. Anatomy of luminosity functions: the 2dFGRS example. *Astronomy and Astrophysics*, 495(1):37–51, February 2009. doi: 10.1051/0004-6361:200810274.

E. Tempel, R. Kipper, A. Tamm, M. Gramann, M. Einasto, T. Sepp, and T. Tuvikene. Friends-of-friends galaxy group finder with membership refinement. Application to the local Universe. *Astronomy and Astrophysics*, 588:A14, April 2016. doi: 10.1051/0004-6361/201527755.

M. Tremmel, A. C. Wright, A. M. Brooks, F. Munshi, D. Nagai, and T. R. Quinn. The formation of ultradiffuse galaxies in the RomulusC galaxy cluster simulation. *Monthly Notices of the Royal Astronomical Society*, 497(3):2786–2810, September 2020. doi: 10.1093/mnras/staa2015.

Neil Trentham, R. Brent Tully, and Andisheh Mahdavi. Dwarf galaxies in the dynamically evolved NGC 1407 Group. *Monthly Notices of the Royal Astronomical Society*, 369(3):1375–1391, July 2006. doi: 10.1111/j.1365-2966.2006.10378.x.

R. Brent Tully, L. Rizzi, A. E. Dolphin, I. D. Karachentsev, V. E. Karachentseva, D. I. Makarov, L. Makarova, S. Sakai, and E. J. Shaya. Associations of Dwarf Galaxies. *Astronomical Journal*, 132(2):729–748, August 2006. doi: 10.1086/505466.

R. Brent Tully, Hélène Courtois, Yehuda Hoffman, and Daniel Pomarède. The Laniakea supercluster of galaxies. *Nature*, 513(7516):71–73, September 2014. doi: 10.1038/nature13674.

A. Vallenari, L. Schmidtobreick, and D. J. Bomans. The star formation history of the LSB galaxy UGC 5889. *Astronomy and Astrophysics*, 435(3):821–829, June 2005. doi: 10.1051/0004-6361:20041138.

Pieter G. van Dokkum, Roberto Abraham, Allison Merritt, Jielai Zhang, Marla Geha, and Charlie Conroy. Forty-seven Milky Way-sized, Extremely Diffuse Galaxies in the Coma Cluster. *Astrophysical Journal Letters*, 798(2):L45, January 2015. doi: 10.1088/2041-8205/798/2/L45.

Aku Venhola. *Evolution of dwarf galaxies in the Fornax cluster*. PhD thesis, University of Groningen, 2019.

Aku Venhola, Reynier Peletier, Eija Laurikainen, Heikki Salo, Thorsten Lisker, Enrichetta Iodice, Massimo Capaccioli, Gijs Verdois Kleijn, Edwin Valentijn, Steffen Mieske, Michael Hilker, Carolin Wittmann, Glenn van de Ven, Aniello Grado, Marilena Spavone, Michele Cantiello, Nicola Napolitano, Maurizio Paolillo, and Jesús Falcón-Barroso. The Fornax Deep Survey with VST. III. Low surface brightness dwarfs and ultra diffuse galaxies in the center of the Fornax cluster. *Astronomy and Astrophysics*, 608:A142, December 2017. doi: 10.1051/0004-6361/201730696.

Aku Venhola, Reynier Peletier, Eija Laurikainen, Heikki Salo, Enrichetta Iodice, Steffen Mieske, Michael Hilker, Carolin Wittmann, Thorsten Lisker, Maurizio Paolillo, Michele Cantiello, Joachim Janz, Marilena Spavone, Raffaele D'Abrusco, Glenn van de Ven, Nicola Napolitano, Gijs Verdoes Kleijn, Natasha Maddox, Massimo Capaccioli, Aniello Grado, Edwin Valentijn, Jesús Falcón-Barroso, and Luca Limatola. The Fornax Deep Survey with the VST. IV. A size and magnitude limited catalog of dwarf galaxies in the area of the Fornax cluster. *Astronomy and Astrophysics*, 620:A165, December 2018. doi: 10.1051/0004-6361/201833933.

Aku Venhola, Reynier F. Peletier, Heikki Salo, Eija Laurikainen, Joachim Janz, Caroline Haigh, Michael H. F. Wilkinson, Enrichetta Iodice, Michael Hilker, Steffen Mieske, Michele Cantiello, and Marilena Spavone. The Fornax Deep Survey with the VST. XII. Low surface brightness dwarf galaxies in the Fornax cluster. *Astronomy and Astrophysics*, 662:A43, June 2022. doi: 10.1051/0004-6361/202141756.

Mark Vogelsberger, Shy Genel, Volker Springel, Paul Torrey, Debora Sijacki, Dandan Xu, Greg Snyder, Dylan Nelson, and Lars Hernquist. Introducing the Illustris Project: simulating the coevolution of dark and visible matter in the Universe. *Monthly Notices of the Royal Astronomical Society*, 444 (2):1518–1547, October 2014. doi: 10.1093/mnras/stu1536.

Yu Wang, Xiaohu Yang, H. J. Mo, Frank C. van den Bosch, Neal Katz, Anna Pasquali, Daniel H. McIntosh, and Simone M. Weinmann. The Nature of Red Dwarf Galaxies. *Astrophysical Journal*, 697(1):247–257, May 2009. doi: 10.1088/0004-637X/697/1/247.

M. Wenger, F. Ochsenbein, D. Egret, P. Dubois, F. Bonnarel, S. Borde, F. Genova, G. Jasniewicz, S. Laloë, S. Lesteven, and R. Monier. The SIMBAD astronomical database. The CDS reference database for astronomical objects. *Astronomy and Astrophysics Supplement Series*, 143:9–22, April 2000. doi: 10.1051/aas:2000332.

Coral Wheeler, Andrew B. Pace, James S. Bullock, Michael Boylan-Kolchin, Jose Oñorbe, Oliver D. Elbert, Alex Fitts, Philip F. Hopkins, and Dušan Kereš. The no-spin zone: rotation versus dispersion support in observed and simulated dwarf galaxies. *Monthly Notices of the Royal Astronomical Society*, 465(2):2420–2431, February 2017. doi: 10.1093/mnras/stw2583.

S. D. M. White and M. J. Rees. Core condensation in heavy halos: a two-stage theory for galaxy formation and clustering. *Monthly Notices of the Royal Astronomical Society*, 183:341–358, May 1978. doi: 10.1093/mnras/183.3.341.

Emílio Zanatta, Rubén Sánchez-Janssen, Rafael S. de Souza, Ana L. Chies-Santos, and John P. Blakeslee. NSCs from groups to clusters: a catalogue of dwarf galaxies in the Shapley supercluster and the role of environment in galaxy nucleation. *Monthly Notices of the Royal Astronomical Society*, 530(3):2670–2687, May 2024. doi: 10.1093/mnras/stae849.

Dennis Zaritsky, Richard Donnerstein, Arjun Dey, Ananthan Karunakaran, Jennifer Kadowaki, Donghyeon J. Khim, Kristine Spekkens, and Huanian Zhang. Systematically Measuring Ultra-diffuse Galaxies (SMUDGes). V. The Complete SMUDGes Catalog and the Nature of Ultradiffuse Galaxies. *Astrophysical Journal Supplement*, 267(2):27, August 2023. doi: 10.3847/1538-4365/acdd71.

Idit Zehavi, Zheng Zheng, David H. Weinberg, Michael R. Blanton, Neta A. Bahcall, Andreas A. Berlind, Jon Brinkmann, Joshua A. Frieman, James E. Gunn, Robert H. Lupton, Robert C. Nichol, Will J. Percival, Donald P. Schneider, Ramin A. Skibba, Michael A. Strauss, Max Tegmark, and Donald G. York. Galaxy Clustering in the Completed SDSS Redshift Survey: The Dependence on Color and Luminosity. *Astrophysical Journal*, 736(1):59, July 2011. doi: 10.1088/0004-637X/736/1/59.